Characterization of the subunit Cβ2 of Protein Kinase A (PKA)

DNA mapping, glucose uptake in KO mice and reaction in T cell activity as a response to incremental concentrations of glucose

Aud Marit Eriksen

Master of Health Sciences,
Institute of Health and Society,
in association with the Institute of Basic Medical Sciences,
Faculty of Medicine,

The University of Oslo (UiO)

14.11.2014

2014

Characterization of the subunit Cβ2 of Protein Kinase A (PKA), DNA mapping, glucose uptake in KO mice and reaction in T cell activity as a response to incremental concentrations of glucose

Aud Marit Eriksen

http://www.duo.uio.no/

Trykk: Copycat, Forskningsparken, Universitetet i Oslo

Abstract

Protein Kinase A (PKA) is a holoenzyme that consists of a regulatory (R) subunit dimer and two catalytic (C) subunits. Genes, which encode the catalytic subunit C, PRKACA and PRKACB, have several splice variants including Cβ2. Cβ2 subunit is highly expressed in T, B and Natural Killer cells. PKA regulates several functions including immune cell proliferation and glucose uptake and metabolism.

We have used mice knocked out for the Cβ2 subunit of PKA. Polymerase Chain Reaction was used to clarify mice genotype and Western Blot analysis to verify ablation of Cβ2 protein in KO mice. Catalytic activity was significantly downregulated by 40 % in Cβ2 KO lymph node, spleen and thymus cells, suggesting that Cβ2 activity could be involved in the regulation of cell proliferation. We therefore used CD3/CD28 coated beads for stimulation of T cells and observed no difference in proliferation rates between Cβ2 KO lymphocytes and wild type cells from mice lymph nodes. Because the results could have been influenced by other cells, we repeated these experiments with positively isolated $CD4^+$ T cells, which verified our previous result. There was, however, a significant increase in proliferation rate in Cβ2 KO spleen cells compared to wt and that was absent in cells isolated from lymph nodes. The biological significance of this observation is unclear. We also found unaltered RIα and RIIα subunit expressions in Cβ2 KO lymph node, spleen and thymus cells and that a mixed T cell population required glucose in order to proliferate. While investigating whether Cβ2 ablation could have an effect on glucose consumption we found this not to be the case. We did, however, find that Cβ2 could possess a regulatory link in the conversion and boosting effect of pyruvate.

Taken into account that catalytic activity was reduced in all tissues but cells maintained their proliferation rate, even under different concentrations of glucose, Cβ2 does not appear to be important for cell proliferation or energy generation.

Acknowledgements

This work has been performed at the Department of Nutrition in cooperation with the Institute of Health and Society, of Basic Medical Sciences at the University of Oslo, in the period of August 2013 to November 2014.

The learning curve in this process has been steep. I have found myself thinking that the writing experience has been quite like when I first went to a drawing class. I drew a kettle how it appeared to me and then someone came and told me that "this is not right, It`s round in the bottom". And just then I saw that I had drawn a straight line. I was eight years old, but the point is still the same. Sometimes you need a support system to tell you something is wrong, before you can see what is right. And like Molière said: "The greater the obstacle, the more glory in overcoming it."

I owe many thanks to my supervising Professor Bjørn Steen Skålhegg, who first of all believed that I could do this, despite my background from public nutrition. Secondly, he has pushed me to study hard and pointed me in the right direction when needed (which was most of the time). Thirdly, for keeping such a good group of people together and making everyone laugh. Thank you.

I could not have done this without Line, my direct supervisor. First of all, she thought me all the methods I have used in this thesis. Secondly, she has given me many advice regarding the writing process; "when writing a thesis, everything is allowed", an advice I have followed every step of the way. Thirdly, she is an excellent brewer and knows her stuff and has naturally awakened my interest in beer. ☺ So thank you Line for the support and help during this time. I am forever grateful.

I would also like to thank Anja, Roman, Tore, Zeynep, Halvor, Henning, Sissel, Aud, Tuva, Claudia and Ken for all your help whenever needed, funny moments, good food, sweet food, drinks, good company and what not! I will miss you, but see you again ☺

Last, but not least, I would like to thank my family, boyfriend and friends. You have cheered me through and given me space. At last, I will see you again!

Aud Marit Eriksen
Oslo, November 2014

ABBREVIATIONS

[3H] - Thymidine	1-(2-deoxy-beta-D-ribofuranosyl)-5 methyluracil
129 V/J	Congenic; Mutant Strain; Targeted Mutation mouse
AC	Adenylyl Cyclase
AKAPs	A-kinase anchoring proteins
Akt	Serine/threonine protein kinase Akt
APC	Antigen-presenting cell
ATP	Adenosine Triphosphate
BMI	Body Mass Index
C57BL/6	Black 6 mouse (wild type mouse)
C	C subunit of PKA
Cβ2	C subunit of PKA
cAMP	cyclic Adenosine Monophosphate
CD3	T cell receptor
CD28	T cell receptor
$CD4^+$	T cell receptor
$CD8^+$	T cell receptor
CoA	Coenzyme A
CRE	cAMP response element
CREB	cAMP response element binding protein
CreER	Cre recombinases bound to Estrogen receptor
Cre-loxP	Cre recombinase / locus of X-over P1
CRP	C-reactive protein
Csk	C-terminal of Src family kinase
DNA	Deoxyribonucleic acid
dNTP	Deoxyribonucleotide Triphosphate
EDTA	Ethylenediaminetetraacetic acid

EP	Prostanoid receptor
Epac	Exchange protein directly activated by cAMP
ERK	Extracellular signal-regulated kinase
ES	Stem cells
FBS	Fetal Bovine Serum
Flp	Flippase
FRT	site sequence
GADPH	Glyseraldehyde 3-poshphate dehydrogenase
GLUT	Glucose transporter
GLP-1	Glucagon like peptide 1
G_q	Glucagon receptor
$G_s\alpha$	Glucagon receptor
GSIS	Glucose-stimulated insulin secretion
HCl	Hydrogen Clorid
HDL	High Density Lipoprotein
HLA	Human Leukocyte Antigen
IL-2	Interleukin 2
IRS-1	insulin receptor substrate-1
K_{act}	Activation constant
kDa	Kilo Dalton
KO	Knockout
LDL	Low Density Lipoprotein
LKB	Liver kinase B1
MHC	Major Hitocompatibility complex
MHCI	Major Histocompatibility complex class I
MHCII	Major Histocompatibility complex class II
mTOR	Mammalian target of Rapamycin

Myc/c-Myc	Transcription factor
NaCl	Sodium Chloride
NaF	Sodium Fluoride
Napp	Sodium Pyrophosphate
Na3VO4	Sodium Vanadate
NARA	National Animal Research Autority of Norway
NCDs	Non-Communicable Diseases
Neo	Neomycin
NEAA	Non-Essential Amino Acids
NF- κB	nuclear factor-κappaB
NK cells	Natural Killer cells
OHT	Synthetic Estrogen Receptor Ligand 4-hydroxytamoxifen
PCR	Polymerase Chain Reaction
PDE	Phosphodiesterase
Pi	Proteinase Inhibitor
PI(3)K	Phosphatidylinositol-3-OH kinase
PKA	Protein kinase A
PKAI	Protein Kinase A type I
PKA II	Protein Kinase A type II
PKI	Protein Kinase Inhibitor
PLCg-1/2	Phospholipase C, gamma 1/2
PMSF	Phenylmethanesulfonylfluoride
PPP	Pentose Phosphate Pathway
PRKAC	Gene of PKA C subunit
P/S	Penicillin Streptomycin
PRKX	Human PKA gene
PTK	Protein tyrosine kinases

PVDF	Polyvinylidene fluoride membrane
R	Regulatory subunit of PKA
SD	Standard Deviation
SDS	Sodium dodecyl sulphate
SEM	Standard Error of the Mean
Src	Family kinase Lck.
TBST	Tris-buffered saline Tween-20
Tc	Cytotoxic T cell
TCA	Tricarboxylic Acid Cycle
Th	T helper cell
T_{eff}	T effector cell
T_{reg}	T regulatory cell
TCR	T cell Receptor
WT	Wild type

Table of content

1 Introduction

1.1 Non-Communicable Diseases

By year 2015, it is estimated that 1.5 billion people will be obese and 41 million deaths will be from chronic diseases (WHO, 2014b, 2014d). A similar trend is seen in Norway. The definition of obesity varies but is normally considered a chronic condition defined by an excess amount of body fat. The normal amount of body fat (expressed as percentage of body fat) is between 25 % - 30 % in women and 18 % - 23 % in men (Muth, 2009). Women with over 30 % body fat and men with over 25 % body fat are considered obese. The calculation of Body Mass Index (BMI; Kg/m^2) has also been used for definition of obesity. Since BMI describes body weight relative to height, it is strongly correlated with total body fat content in adults. "Obesity" is defined as a BMI of 30 and above (WHO, 2014a, 2014c). In 2005 The Norwegian Institute of Public Heath (fhi.no) estimated that about 20 % of men and 17 % of women in Norway were obese, with BMI above or equal to 30 (Hånes, 2014).

Obesity is often associated with the metabolic syndrome also known as Syndrome X, insulin resistance syndrome, and dysmetabolic syndrome. These are characterized by a group of metabolic risk factors which include, abdominal obesity (excessive fat tissue in and around the abdomen (waist circumference men > 102 cm and woman > 88 cm), atherogenic dyslipidaemia (blood fat disorders — high triglycerides (> 150 mg/dL), low HDL (< 40 (men) and < 50 (women) mg/dL) cholesterol and high LDL cholesterol — that foster plaque build-ups in artery walls), elevated blood pressure (> 140/90 mmHg), insulin resistance and glucose intolerance (> 100 mg/dL), and prothrombotic state (e.g. high fibrinogen or plasminogen activator inhibitor–1 in the blood) (Powers, 2005; Zimmet, Alberti, & Shaw, 2001). The most common lifestyle cause of obesity is the over-consumption of energy dense foods such as animal fats, cured salted meats and lack of vegetables as well as lack of physical activity (Bremer, Devaraj, Afify, & Jialal, 2011; Bremer & Jialal, 2013; Palomer, Salvado, Barroso, & Vazquez-Carrera, 2013). There is growing evidence that links obesity to chronic low-grade inflammation, metabolic dysregulation and cytokine production (Bremer et al., 2011; Bremer & Jialal, 2013; Emanuela et al., 2012; Esser, Legrand-Poels, Piette, Scheen, & Paquot, 2014; Johnson, Milner, & Makowski, 2012; McLaughlin et al., 2014; Palomer et al., 2013). This is supported by the fact that obese people show another hallmark of disease, increased levels of

C-reactive protein (CRP > 10 mg/L) that is indicative of a pro-inflammatory state (Yudkin, Stehouwer, Emeis, & Coppack, 1999). Emanuela et al., (2012) suggest that inflammatory factors are released into the bloodstream after a meal. Whereas these factors seem to resolve in slim individuals, in obese people they appear to accumulate over time and may develop into chronic inflammation (Emanuela et al., 2012). A state of chronic inflammation in obesity is also consistent with the development of several comorbidities in obesity such as diabetes type 2, cardiovascular disease and cancer which are all chronic non-communicable diseases (NCDs) (Esser et al., 2014; Johnson et al., 2012; Palomer et al., 2013).

1.2 The immune system

The ability of the immune system to successfully combat infectious agents without causing undue harm to the surrounding tissues depends on its capacity to distinguish between foreign and self. This requires high discriminatory power and tight control, that when lost may lead to a broad spectrum of diseases categorized as inflammatory. Pro-inflammation or low grade chronic inflammations which have been thought to be beneficial to the host could also contribute to several infectious diseases. Pro-inflammation is a causal factor in the development of diabetes and atherosclerosis, which are characteristics of metabolic syndrome (Figure 1.). The system is in large part divided into the innate and the adaptive immune system, working together to protect the body (Lea, 2008).

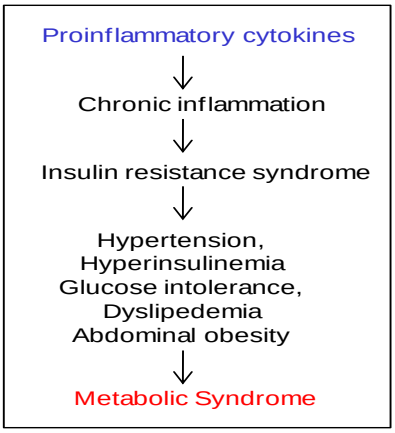

Figure 1. Development of the Metabolic Syndrome X
A representation of the cascade of immunological events, starting with pro-inflammatory cytokines and ending with the development of Metabolic Syndrome X.

1.2.1 The innate immune system

The innate immune system consists of the skin, sweat and tears, mucosa, low pH in the stomach and bacteria in the gut. Together they form the outer line of defence. The inner line of defence includes phagocytes (monocytes, macrophages, and granulocytes), dendritic cells, mast cells and Natural Killer cells (NK cells). If microorganisms are able to pass, a humoral

part is set in motion. The humoral part of the innate immune system contains all soluble components that exist in body fluids and function as a line of defence against infections. It consists of acute phase proteins, the complement system and interferons. The innate immune system is the first line of defence, and responds quickly. The phagocytes surround and absorb the microorganisms and destroy it by releasing substances that kills the microorganism. The macrophages are also able to assist the adaptive immune system by helping to recognize and react to foreign substances (Lea, 2008).

1.2.2 The adaptive immune system

The adaptive immune system is developed during the first year of living and consists of B and T lymphocytes and NK cells. The immune response is divided into two parts, the humoral and cellular part (Lea, 2008). The main function of the humoral part is the production of antibodies, and the processes that follows, like T helper cell activation but also cytokines production, affinity maturation and generation of memory cells (T cell development will be explained further). The cellular part involves activation of phagocytes, antigen specific cytotoxic T lymphocytes and the release of various cytokines in response to an antigen. An antigen is a relatively big molecule that is recognized by an antibody (Lea, 2008). An effective immune system requires that the innate and adaptive, the humoral and the cellular components function together.

Maturation of B and T cells

All mammals have genes that encode molecules crucial for recognition of antigen and subsequent immune response. The gene complex Major Histocompatibility Complex (MHC) is located on chromosome six in humans in an area called the Human Leukocyte Antigen (HLA) region. The genes from the HLA area codes for HLA antigens and HLA molecules and codes for class I, II and III glycoproteins. Class I and II are tissue- or transplantation antigens, and class III are free molecules in plasma. MHC molecules function as information transport proteins and present the foreign peptide structure on the cell surface, communicating to the surrounding cells about the inner activities of the cell (Lea, 2008).

All immune cells are produced in the bone marrow. B cells then mature in secondary lymphoid organs such as the lymph nodes and the spleen. T cells are released as immature

thymocytes that populate the thymus for further maturation (figure 2). Once matured, the B and T lymphocytes are equipped with special membrane bound receptors, which makes them capable of recognizing different antigen structures that can bind antibodies. When a B lymphocyte antibody binds to an antigen, it differentiates. Some cells become plasma cells that produce new antibodies, and others become memory cells. Antibodies, known as immunoglobulins, are Y-shaped proteins produced by plasma cells. Their function is to bind to a small part of the antigen. MHC molecules are on antigen presenting dendritic cells (APC). T cells have T cell receptors CD4 or CD8 molecules which bind MHC II or MHC I respectively (Lea, 2008).

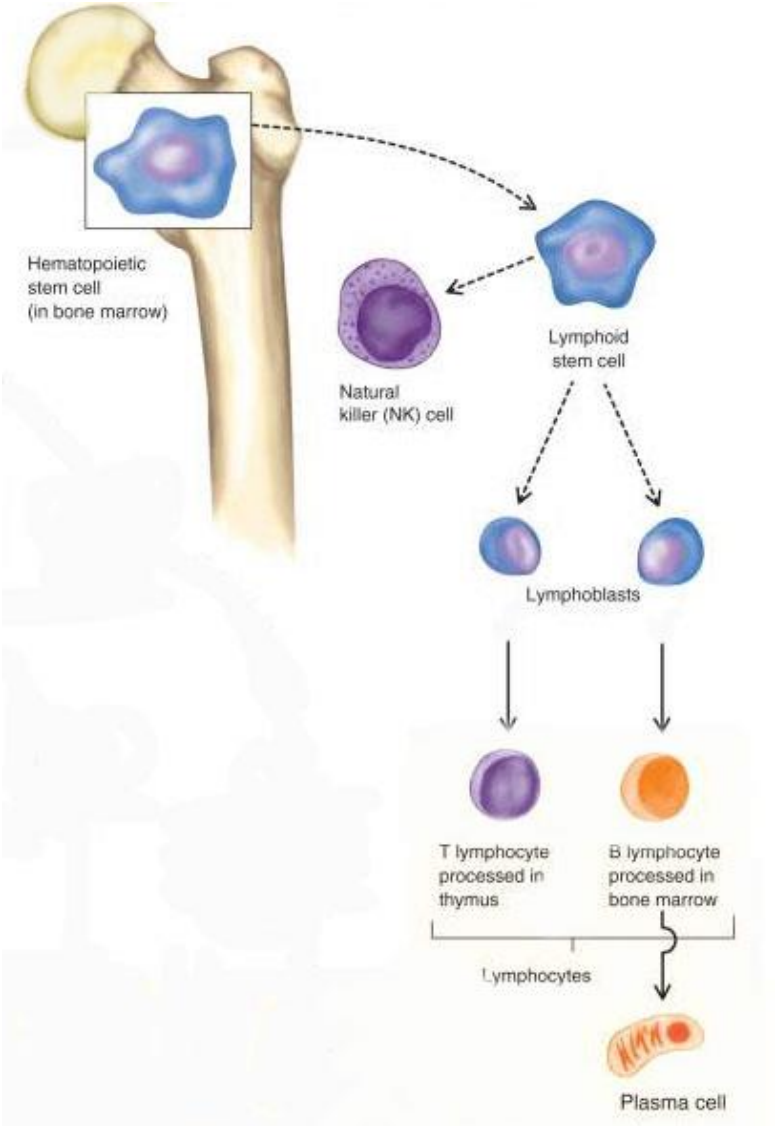

Figure 2. The development of stem cells intoT and B lymphocytes
A presentation of stem cells developing in the bone marrow, and becoming T and B cells as well as Natural Killer cells. B cells are fully functional when leaving the bone marrow while T cells develop further in the Thymus (Lea, 2008).

Tolerance and autoimmunity

During maturation in the thymus, different genes that code for antigen receptor polypeptide chains cause a variety of structural differences. T cell receptors can recognize virtually any imaginable structure, including the body's own. However, it should only react to foreign structures. T cells that interact with MHC-I or MHC-II are first selected through a process called positive selection, where the cells that do not bind, die. Secondly, the cells pass through a negative selection process where those that bind too strongly to the MHC complex receive an apoptotic signal, leading to cell death. A defective selection process could lead to immunological tolerance meaning that the immune system could attack the body´s own autologous antigens, causing an autoimmune disease, like diabetes type 1 (Lea, 2008).

While B lymphocytes supervise the extracellular compartment, T cells control the intracellular compartment with help from the MHC molecules. From this point on, this thesis will primarily focus on T lymphocytes.

Activation of T cells

T cells need to be presented with an antigen on the surface of an APC with MHC class I molecules or class II. As mentioned, CD4 molecules bind to MHC II and CD8 molecules bind to MHC I, respectively. Further, all T cells have CD3 recognition markers on the cell surface, which transfer the activation signal from the T cell receptor (TCR) over the membrane and into the cell. The intracellular parts are then phosphorylated by protein tyrosine kinases (PTK), which signals the cell to start dividing. Alongside CD3 are co-receptors that contribute to the activation process as CD28. For T cells to evolve into effector cells, they need activation signals from both CD3 and CD28. The TCR recognizes the associated ligands presented by the MHC molecule on the APC. The signal from CD28 engages T cells triggering Interleukin 2 (IL-2) production, which triggers T cell activation (Lea, 2008; Maciolek, Pasternak, & Wilson, 2014).

Once activated, T cells differentiate from naïve into different subsets based on their capability to act cytotoxic, engage in a helper or a regulatory function (figure 3). Cytotoxic cells (Tc, $CD8^+$) when activated, results in a rapid proliferation as part of the clonal expansion phase (Bannard, Kraman, & Fearon, 2009). $CD8^+$ secretes pro-inflammatory cytokines (Tumor Necrosis Factor α and Interferon γ) and lysate targeted cells. Once the immune system has

eliminated the pathogens, Tc cells die. However, a small population remains as T memory cells which has rapid recall ability (DiSpirito & Shen, 2010). Naïve $CD4^+$ cells develop into T helper cells; Th_1, Th_2, and Th_{17}, effector cells (T_{eff}) and T regulatory cells (T_{reg}). T helper cells are essential for the adaptive immune system. They release cytokines and suppress or regulate an immune response. T_{reg} cells, also known as suppressor T cells, shuts down T cell mediated immunity towards the end of an immune reaction and maintain tolerance to autologous antigens (Sakaguchi, Miyara, Costantino, & Hafler, 2010).

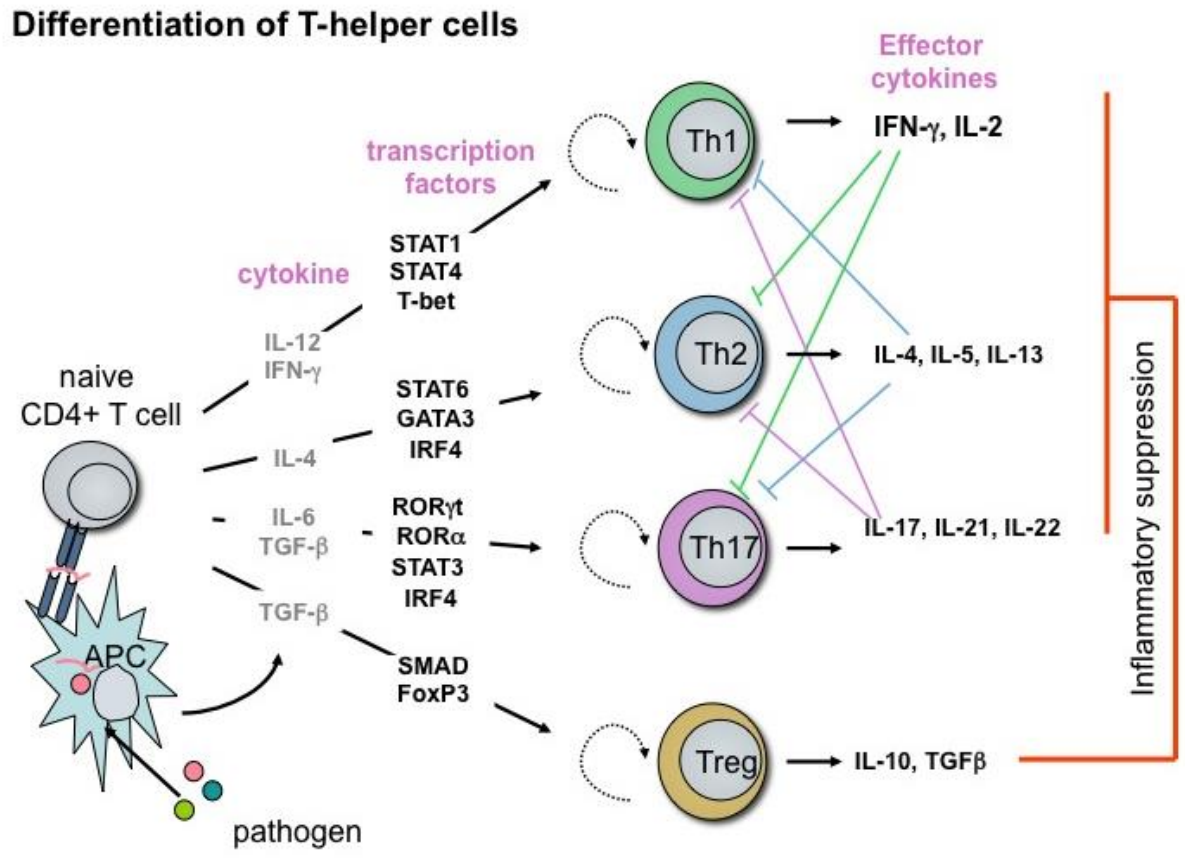

Figure 3. Development of T cells
A schematic presentation of T cells development into functional T helper cells (Th_1, Th_2, Th_{17}) and T_{reg} cells after being represented with MHCII molecules on an APC presenting cell. APCs have a high affinity to TCR on naïve CD4 cells. The recognition of the pathogen by CD4 T cells activates the cells, and they differentiate into T helper cells. Furthermore, the activation is followed by cytokine secretion and specific Th differentiation (Lea, 2008).

Metabolism in T cells

A resting T cell needs primarily Adenosine Triphosphate (ATP) to maintain basal functions. The activation of T cells result in functional changes depending on cell phenotype, preconditioning and present context. This demands energetic and biosynthetic upregulation,

achieved by uptake of nutrients and increased metabolic turnover and flux. The phases of activation are followed by cell death and memory capabilities (Gerriets & Rathmell, 2012; Macintyre et al., 2014; Maciolek et al., 2014; R. Wang & Green, 2012).

The metabolism in lymphocytes are regulated by increased glycolytic flux and lactate production, in addition to elevated production of lipids, proteins, nucleic acids, proteins and other carbohydrates. If glucose is not present in excess, the majority of glucose will flux towards the Tricarboxylic Acid Cycle (TCA) instead of production for biosynthesis (figure 4). If there are ample amounts of glucose, there is an increased flux towards the Pentose Phosphate Pathway (PPP) for nucleotide synthesis, amino acid production and lipid synthesis in order to produce biomass (Frauwirth et al., 2002). Oleszczak, Szablewski and Pliszka (2012) suggest that if glucose is limited, glycolytic flux decreases to a level that supports cell death, but also, that excessive glucose uptake can promote a hyperactive immune response followed by possible pathology (Oleszczak, Szablewski, & Pliszka, 2012). Their evidence has later been reproduced by other researchers (Palmeira, Rolo, Berthiaume, Bjork, & Wallace, 2007). This points out that a close regulation of glucose uptake is required to maintain immune homeostasis.

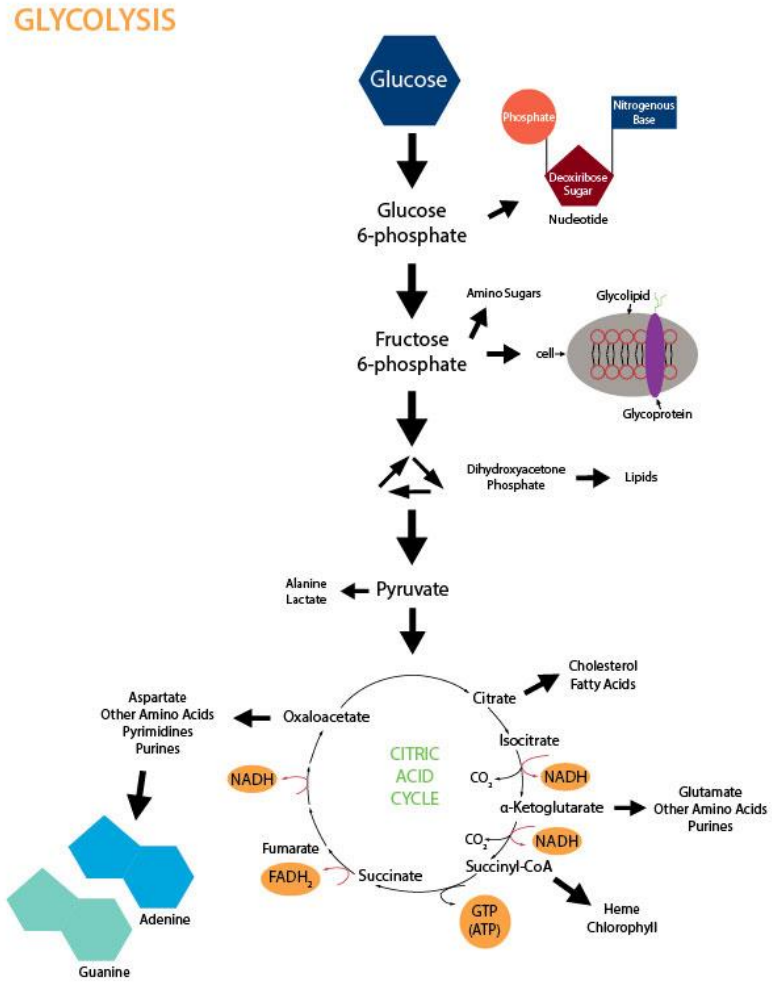

Figure 4. Glycolysis and the tricarboxylic acid cycle (TCA)
The figure illustrates the glycolysis and the breakdown of a glucose molecule into pyruvate and the entering to the TCA cycle. From here, the model shows how the substrate can be used further, such as cholesterol, glutamate, amino acids etc. (Maciolek et al., 2014).

Glucose breaks down to pyruvate through the steps of glycolysis. Pyruvate is then converted to ATP through the glycolytic pathway (Maciolek et al., 2014). Pyruvate is by many researchers considered extra fuel, and Sena et al. (2013) found that adding sodium pyruvate to the cells could recover the cells viability (Sena et al., 2013).

Based on the availability of oxygen, pyruvate may be converted to acetyl-CoA and enter the TCA cycle. Nicotinamide Adenine Dinucleotide and Flavin Adenin Dinucleotide produced by the TCA cycle provide electrons to the Electron Transport Chain. This process produces 32 molecules of ATP and six molecules of Carbon Dioxide. When oxygen is limited, mitochondrial oxidative metabolism becomes restricted, and pyruvate converts to lactate by the enzyme Lactate Dehydrogenase. This production generates two ATP molecules per glucose molecule (Finlay & Cantrell, 2011; Jacobs et al., 2008; O'Neill & Hardie, 2013).

THE ROLE OF GLUCOSE IN LYMPHOCYTES

Glucose enters the lymphoid cells across the plasma membranes through the GLUT 1 glucose transporter, as a response to the increased demand for rapid fuel. This appears as an early event in T cell activation. CD28 stimulation signal acts through Phosphatidylinositol-3-OH kinase (PI(3)K)-Akt and the mammalian target of rapamycin (mTOR) signalling and promotes GLUT 1. Combined, GLUT 1 protein levels and Akt signalling enhances glucose uptake and T cell activation (Frauwirth et al., 2002; Jacobs et al., 2008; Macintyre et al., 2014).

Macintyre et al. investigated the role and mechanisms that control glucose uptake and metabolism in T cells. They found that GLUT 1 has a selective cell-characteristic function for metabolic regulation of aerobic glycolysis for optimal growth, survival, and proliferation in both murine and human T cells (Macintyre et al., 2014).

Previous studies have also indicated that ERK, - Akt-, and mTOR-mediated signalling pathways are involved in T cell metabolism (Carr et al., 2010; Frauwirth et al., 2002; Pearce et al., 2009). Wang et al. propose that these pathways could regulate T cell metabolism partially through the transcription factor cMyc and Hypoxia-inducible factor 1-alpha, which was supported by others (Keith, Johnson, & Simon, 2012; Semenza, 2012; Shi et al., 2011; R. Wang et al., 2011). Wang et al. suggest that Myc is required for the induction of enhanced glycolytic activity and metabolic gene expression in T cells (R. Wang et al., 2011). In addition, Estrogen related receptor α is also proposed as a transcription factor that regulates T cell metabolism (Frauwirth et al., 2002; Macintyre et al., 2014; Michalek et al., 2011).

Otto Warburg discovered that aerobic glycolysis predominates in cancer cells even when oxygen is abundant. This process is called the "Warburg effect" (Vander Heiden, Cantley, & Thompson, 2009; Warburg, Wind, & Negelein, 1927). There are differences and similarities between activated T cells and the metabolic change in tumours. The differences being that inflammation is driven by extracellular signals and tumour cells are caused by mutations (Frauwirth et al., 2002; O'Neill & Hardie, 2013) and the similarities being that both have roles in regards to PI3K-Akt-mTOR as a pathway for c-Myc (R. Wang et al., 2011). Activated T_{eff} cells have shown a shift towards high glycolysis which could be a sign of inflammation,

whereas T_{reg} cells have shown a shift towards oxidative phosphorylation and could be a sign of anti-inflammatory cells (O´Neill & Hardie, 2013).

Insulin directly influences T cell metabolism and immunity. T cells express the insulin receptor in response to antigen activation (Stentz & Kitabchi, 2003). Further, activated T cells respond to the hormone by increasing IL-2 expression and increased phosphorylation of the insulin receptor substrate-1 (IRS-1) (Saucillo, Gerriets, Sheng, Rathmell, & Maciver, 2014; Stentz & Kitabchi, 2003; Viardot et al., 2012). Insulin triggers activated T cells to increase the consumption of glucose and amino acids, increase glycolytic flux and protein synthesis, increase flux via the PPP and promote anti-inflammatory environment by stimulating differentiation of more T_{H2}-type $CD4^+$ and cytokines (Bental & Deutsch, 1993; Brown, Ercolani, & Ginsberg, 1983; Ercolani, Lin, & Ginsberg, 1985; Fox, Hammerman, & Thompson, 2005; Kaneto et al., 2001; Stentz & Kitabchi, 2003; Viardot et al., 2012; F. Wang et al., 2012). Insulin resistance in humans impairs T cell function (Stentz & Kitabchi, 2003). Obesity is characterized by insulin resistance and low grade inflammation (Viardot et al., 2012). Viardot et al (2012) presented increased activation markers on neutrophils, monocytes, T lymphocytes as well as a pro-inflammatory type 1-phenotype of T cells (T_{H1})(Viardot et al., 2012). This suggests that nutrient availability and an incorrect response to metabolic hormones could influence T cell function (Viardot et al., 2012).

It is also emerging evidence that leptin, a hormone secreted by white adipocytes, is important for maintenance of body weight as it signals the hypothalamus about satiety (Saucillo et al., 2014), could affect glucose homeostasis and T cell function through promoting T_{H1} and T_{H17} cell differentiation and function while inhibiting T_{reg} proliferation. When nutrient levels are adequate, leptin signals through the T cells Leptin Receptor provides for full T cell activation (Cham & Gajewski, 2005; Papathanassoglou et al., 2006; Procaccini, Jirillo, & Matarese, 2012; Saucillo et al., 2014; Yu et al., 2013).

There is need for further research on the topic of glucose uptake, metabolism and inflammatory disease. Understanding the roles and regulation of specific nutrient transporters in T cell activation and subsets may provide opportunities to exploit metabolic distinctions of cells in the immune system to control inflammatory diseases.

1.2.1 Protein Kinase A

A key regulator of both glucose and lipid metabolism and lymphocyte activity is the tetramer holoenzyme Protein kinase A (PKA), type I and II. The enzyme is activated in response to an increase in cyclic Adenosine Monophosphate (cAMP) in the cell (Ane Funderud et al., 2009; Skalhegg et al., 2005). PKA consists of a regulatory (R) subunit dimer and two catalytic (C) subunits, which together constitutes of PKA in an intact form. When levels of cAMP rises, four molecules of cAMP bind to the R subunits, causing a conformational change that releases the two C subunits. There are four known R subunits designated RIα, RIβ, RIIβ, RIIα and RIIβ, and four C subunits designated Cα, Cβ, Cγ and PRKX (Skalhegg & Tasken, 2000). PKAI is composed of $RI\alpha_2C_2$ or $RI\beta_2C_2$ and PKA II is composed of $RII\alpha_2C_2$, $RII\beta_2C_2$. PKAI and PKAII are activated with an activation constant (K_{act}) for cAMP of 50-100 nM and of 200-400 nM, respectively. The C subunit phosphorylates threonine and serine residues on target proteins (Skalhegg et al., 2005).

The PRKX differs from Cα and Cβ, who are quite similar isoforms (Oksvold et al., 2008). The human Cα gene encodes Cα1 and Cαs/Cα2. For Cβ at 16 different splice variants have been identified in humans; Cβ1, Cβ2, Cβ3, Cβ4, Cβ4ab, Cβ4abc, Cβ3ab, Cβ3abc, Cβ3b and Cβ4b (Guthrie, Skalhegg, & McKnight, 1997; Kvissel et al., 2004; Orstavik et al., 2001; Uhler, Carmichael, et al., 1986; Wiemann, Kinzel, & Pyerin, 1991). The catalytic subunits Cα and Cβ and their splice variants are encoded by variable N-terminal ends in which the non-identical sequences are encoded by different exons upstream of exon 2 (Figure 5) (Skalhegg et al., 2005).

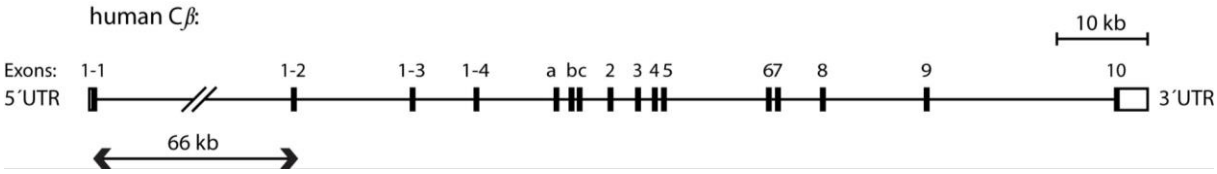

Figure 5. The human Cβ gene.
The figure shows the intronic sequence with exons 1-1 and 1-10. In Cβ2 ablated mice, exon 1-2 is removed by Cre recombinase.

Cα and Cβ and their respective splice variants are tissue specific. The isoforms Cβ3, Cβ4, Cβab, Cβ3b, Cβ3abc, Cβ4ab, Cβ4b, Cβ4abc are all expressed specifically in nerve cells (Kvissel et al., 2004; Orstavik et al., 2001). Studies by Funderud et al. show that a mutation of the CB gene does not result in any clear phenotype and mice appear healthy and fertile.

However, early postnatal lethality has been seen in mice with ablated Cα gene, and amongst those who grew up, male adults appears infertile. Both sexes show a reduction in size of 30 % (Oksvold et al., 2008).

Cα1 and Cβ1 appear ubiquitously expressed, while Cα2 is only expressed in the sperm cells. Cβ2 is highly expressed in lymphoid tissues (Skalhegg et al., 2005; Uhler, Chrivia, & McKnight, 1986). Cα1 and Cβ1 isoforms and human Cβ2 have a relative molecular mass of approximately 40 kDa and 47 kDa, respectively, and 47 kDa was restricted to lymph nodes, thymus and spleen. Their study revealed that Cβ contributes significantly to PKA activity in mouse spleen cells (A. Funderud et al., 2006).

PKA and regulation of the immune system

It is established that PKAI regulates the activation of T and B lymphocytes and NK cell cytotoxicity (Levy et al., 1996; Skalhegg et al., 1992; Skalhegg et al., 1994; Torgersen et al., 1997). However, Scillace et al. (2005) have suggested that the RIIα subunit is not required for normal immune functions and that other proteins could be compensating for lack of the subunit when it is ablated in mice (Schillace et al., 2005).

After T and B cells are activated, several intracellular signalling molecules including PTKs, protein tyrosine phosphatases, G-proteins, lipid rafts and adaptor molecules are regulated as a response to the stimulation of TCR CD3/CD28 complex. Together they form a signalling cascade, which takes place in the plasma membrane of lipid rafts (Schwencke et al., 1999; Skalhegg et al., 2005).

Extracellular hormones, like glucagon, or pro-inflammatory factors, like Phosphodiesterase's (PDEs), target G-protein coupled seven-putative transmembrane segments, equipped with prostanoid receptors EP_2 and EP_4. The receptors mediate their action through activation of Adenylyl Cyclase (AC), which in turns ATP to cAMP, activating the cAMP pathway, releasing active C subunits from the holoenzyme PKA (Figure 6). These inflammatory mediators can decrease expression and production of IL-2, because of their inhibiting function on cAMP (Skalhegg et al., 2005).

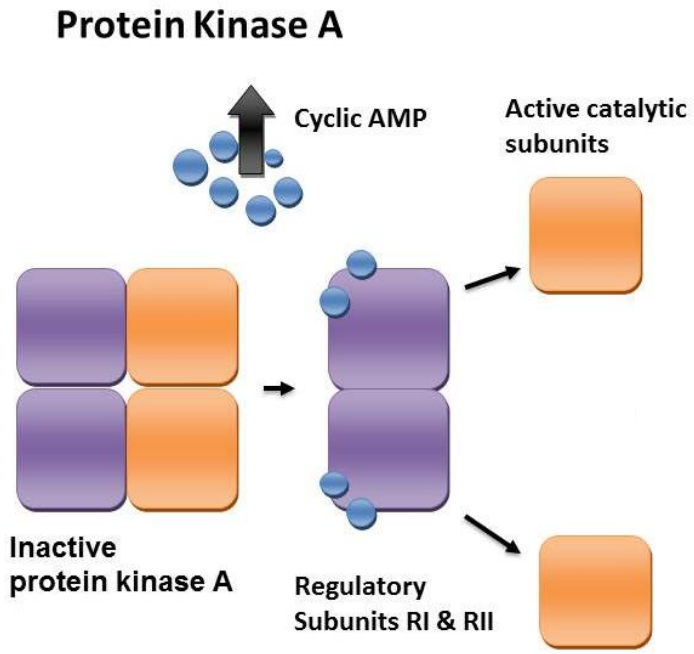

Figure 6. Activation of Protein Kinase A (PKA)
Protein Kinase A (PKA), a tetramer holoenzyme composed of a regulatory (R) subunit dimer bound to two catalytic (C) subunits is activated by endogenous cyclic adenosine monophosphate (cAMP). The purple and orange boxes represent the R and C subunits, respectively, and the blue dots represent cAMP.

A-kinase anchoring proteins (AKAPs) serve as essential points between a diverse set of signalling pathways. AKAPs contain PKA anchoring domains, which bind the R subunit. AKAPs bind ACs and PDEs, which allows for a close regulation of PKA activation and modulation of the immune system (figure 7) (Levitzki, 1988; Skalhegg et al., 2005). In T and B cells, 80 % and 20 % of the soluble PKAI, and the Golgi centrosomal PKAII are anchored through AKAPs, respectively (Skalhegg et al., 1992).

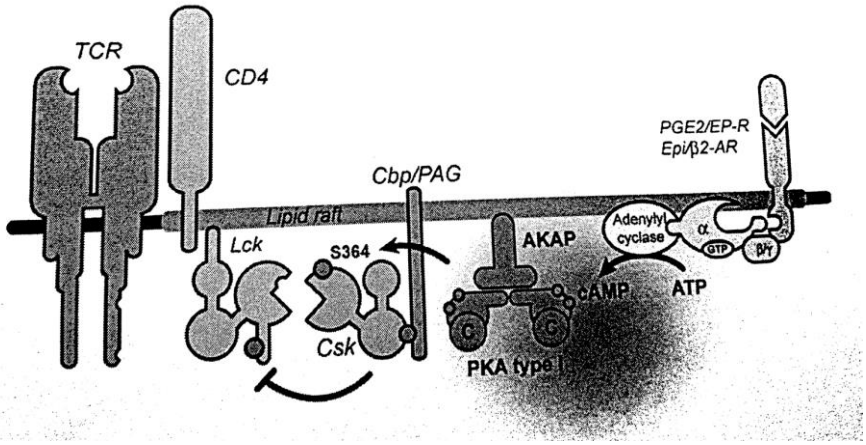

Figure 7. cAMP inhibits T cell activation by PKA.
In T-cells, cAMP have an inhibitory effect on T cell activation through the receptor G protein-AC-cAMP-PKA type I-Csk inhibitory pathway. This takes place in lipid rafts and acts through Src-family kinase LCk, EP-R, prostaglandin E_2 receptor. Also, free catalytic subunits affect the production of IL-2 which regulates the T cell activation.

PKA I phosphorylation affects several components. The inactive C-terminal of Src family kinase (Csk) turns active after signalling from the TCR, to Src family kinase Lck (Skalhegg et al., 2005; Tasken & Aandahl, 2004). Csk regulates TCR-mediated signal transduction as an early event of the activation cascade. Another component is the phosphorylation and regulation of NF-κB and CRE elements (cAMP Response Element). They regulate early and late stages of T cell activation, which are found in several genes (TCR, CD3 and IL2). The CREB (cAMP Response Element Binding protein) binds to CRE, which controls genes involved in cell growth and proliferation. Further, PLCg-1/2 is phosphorylated after stimulation with cAMP elevating agents such as PGE2, which leads to suppression of Calcium mobilization and phosphatidylinositol hydrolysis upon T cell activation (Skalhegg et al., 2005).

Tight regulation of cAMP and PKA is important for a regulative and functioning immune system. Previous research has found that hypoactive PKA could be linked to Systemic Lupus Erythematosus[1] and hyperactive PKA to Human Immuno-deficient virus[2]. Furthermore, the Cβ2 subunit was suggested to be a target for therapeutic treatment (Kammer, 2002; Skalhegg et al., 2005).

PKA, cAMP and metabolic regulation in mammals

The PKA signalling system is ubiquitously expressed and regulates cellular metabolism in many organs, for instance the liver, where PKA regulates both glucose and lipid metabolism. In addition, PKA is involved in insulin and glucagon regulation in the pancreas (London et al., 2014; Saltiel & Kahn, 2001; Schreyer, Cummings, McKnight, & LeBoeuf, 2001; Skalhegg et al., 2005; Tasken & Aandahl, 2004).

Insulin is a polypeptide hormone synthesized by the β-cells in pancreas and regulated by blood glucose levels, which are normally in the range of 4-7 mM (Frayn, 2003; Saltiel & Kahn, 2001). Insulin is also released by secretion of amino acids and ketone bodies. Circulating insulin directs its effect on cells by binding to specific insulin receptors. The hormone glucagon is secreted from the α-cells in the pancreas and released by a fall in

[1] Systemic Lupus Erythematosus (SLE) is a chronic inflammation disease in the connective tissue, with symptoms in the skin and skeleton amongst others (nhi.no, 2013b).
[2] Human Immuno-deficient virus (HIV) is a retrovirus which effects the immune system by breaking it down, making it accessible to other infectious diseases (nhi.no, 2013a).

glucose concentration in plasma, having the opposite effects of insulin (Frayn, 2003; Saltiel & Kahn, 2001). In response to increased gluconeogenesis in the liver, glucagon activates PKA (Foretz, Carling, Guichard, Ferre, & Foufelle, 1998; Jiang & Zhang, 2003; Ouedraogo et al., 2006). Ouedraogo et al. show that glucagon signalling in the liver involves activation of a PKA/LKB/AMPK pathway upstream of mTOR (Ouedraogo et al., 2006). Glucagon can bind to the glucagon receptor ($G_s\alpha$ and G_q) in the membrane. The activation of $G_s\alpha$ is followed by activation of AC and an increase in cAMP, thereby activating PKA. There is also evidence that glucagon like peptide 1 (GLP-1) potentiates glucose-stimulated insulin secretion (GSIS) by elevation of cAMP in pancreatic β-cells, activating PKA. Through activation of cAMP-PKA and cAMP-Epac[3] pathways, GLP-1 stimulates insulin secretion in β-cells at normal glucose concentrations (Luo et al., 2013).

A low level of insulin is followed by an increase of glucagon and gluconeogenesis, which increases the hepatic production of glucose. In addition, the supply of amino acids increases because of net breakdown of protein. Glucose no longer enters the cells and the glucose concentration in plasma rises above normal levels. When a person has a poor glucose tolerance (< 12 mM), the diagnosis is Diabetes Mellitus, which is generally divided in two major forms, type 1 and type 2. Type 1 is defined by loss of insulin-producing cells and has a major genetic, and thus a hereditary component. Type 2 has a genetic component, however, is mostly regarded as a lifestyle created disease. Chronic hyperglycaemia (glucose in plasma above 12 mM) or glucotoxicity leads to damaged β-cell functions that may reduce insulin secretion in both rodents and humans (Cochran et al., 2014; Frayn, 2003).

It is well established that PKA regulates both glucose and lipid metabolism and that PKA play an important role in the activation of T cells. However, the subject of PKA and glucose consumption in T lymphocytes is still not investigated. In order to better understand the role of the splice variant Cβ2 of PKA and glucose consumption; we used a Knockout line (KO) of Cβ2 of PKA. This allowed us to understand more about the possible effects of Cβ2 in respect to the immune system and glucose consumption.

[3] Epac is a cAMP effector protein responsible for PKA stimulatory effects of GLP-1 on insulin secretion at physiological glucose concentrations (Luo et al, 2013).

1.2.2 The Knockout approach

The mice strain is on a C57BL/6:129SV/J genetic background and is KO for Cβ2 of PKA. The project was approved and registered by the National Animal Research Authority of Norway (NARA).

In order to study the biological function of Cβ2, a mouse model ablated for this C subunit was developed by the Skålhegg laboratory in collaboration with genOway (http://www.genoway.com/; see attached booklet in Appendix B for details). In short, a DNA construct for homologous recombination was introduced to embryonic stem (ES) cells that were on an Agouti-129Sv/Pas background. The ES cells were selected for the mutation by resistance to the antibiotic neomycin (neo) and were thereby microinjected into host blastocysts. Blastocysts were then introduced to pseudo pregnant (hormone treated) female mice on a C57BL/6J background. The agouti gene was introduced to assure incorporation of the construct into offspring, as pups carrying this genotype would carry coat colour chimerism. The agouti coat colour (yellow) is dominant over the black coat color. Hence, offspring carrying the mutation would have a mixed yellow/brown/black coat colour. To ensure introduction of the mutation into the germ cell genome, further breeding was performed with male mice with high chimerism (> 85 %) (Figure 8).

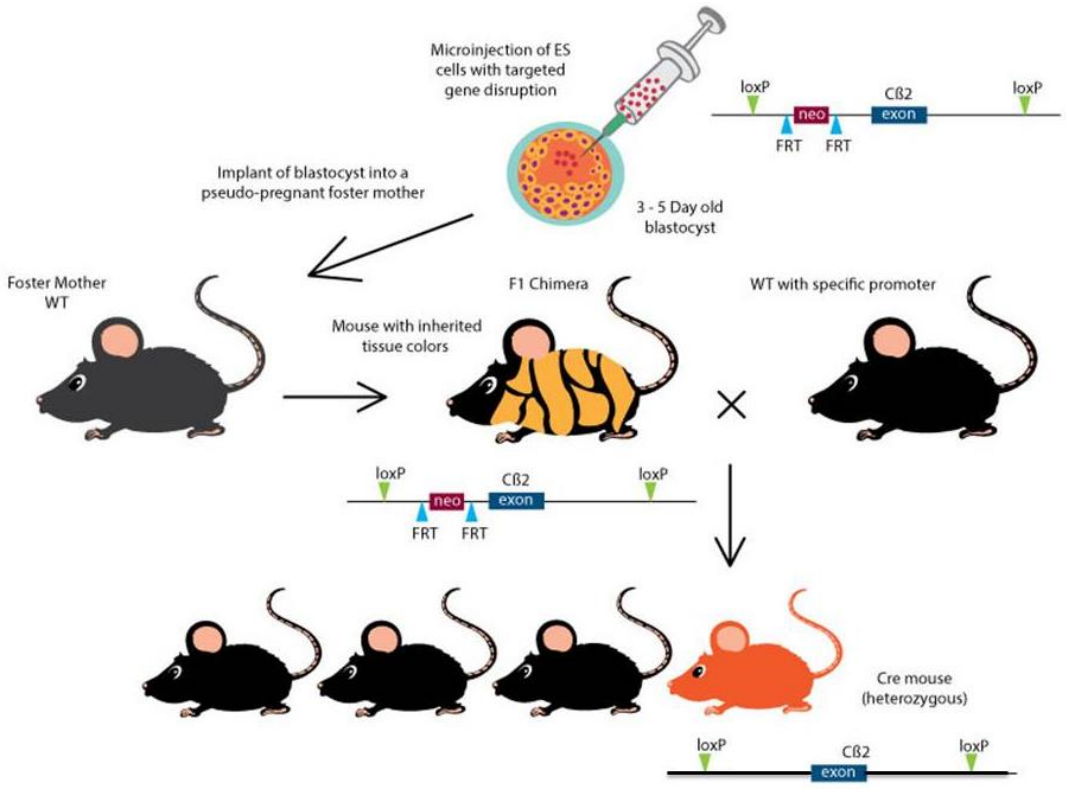

Figure 8. Principle of the conditional KO approach
Once a DNA vector has correctly been incorporated into the genome of embryonic stem (ES) cells, they are injected into 3-5 days old mouse blastocysts. These blastocysts are then injected into a pseudo-pregnant foster mother (dark gray mouse), where the pregnancy has been induced by by hormones. The embryos are then allowed to come to term and because the ES cells and the blastocysts are from two different coloured mice, the pups with two colours (F1) are the evidence of a successful recombination. The final F1 chimeras breed mice with the heterozygote Flp or Cre expressing mice (black mouse) with a possibility for heterozygous pups as result (orange mouse). The blue boxes represents the 1β2 exon of the PKACβ2 isoform. Solid line represents intronic sequences. The LoxP (Cre selection site) and FRT (Flp selection site) elements are shown as green and light blue triangles. Antibiotic (Neo) resistance sites (red boxes) represent the neomycin positive selection cassette.

Further development of the PKACβ2 KO by genOway was to cross these mice with flp-deleter mice on a C57BL/6J background in order to delete the neo cassette which was introduced with a FRT site on each side (figure 8). These mice were heterozygote for the 1β2 exon with a loxP site on each side (Figure 8). These mice were mated to homozygosity for the 1β2-loxP construct followed by specific deletion of exon 1β2 by crossing with a cre-deleter mouse on a C57BL/6J background, which carried active Cre in all known cells and tissues. In this way, there were healthy and fertile mice on a > 75 % C57BL/6J background (tested by Norwegian Transgen Centre) carrying a homozygote null-mutation for Cβ2 (Figure 9).

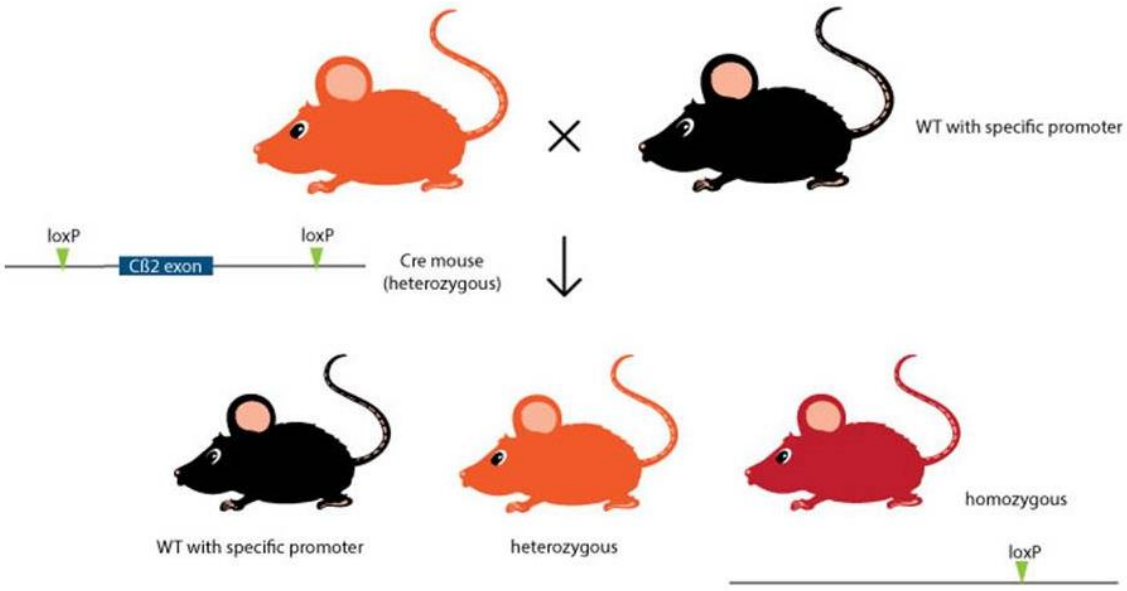

Figure 9. Generation of Cβ2 KO mice
The figure represents the marked loxP sites flanking the exon 1β2 (orange mouse on the upper left side) allowing their deletion under the Cre-recombinase action. Mice breeding with the Flp deleting mice (black mouse on the upper right side), deleted the neomycin box from the exon, creating mice just with the floxed Cβ2 heterozygote. Breeding the Flp mice with the Cre-expressing mice or the floxed Cβ2 heterozygote mice generated PKACβ2 KO animals (red mouse on the right side).

2 Aim and objectives

In order to determine a potential link between Cβ2 of PKA, glucose sensitivity and consumption and T cells, a knockout approach was used. The major aim for this Master Thesis was to determine the following objectives:

Objectives

- Expression and activity of Cβ2 protein in KO mice.
- Characterize PKAR- and C-specific activities for the catalytic subunit Cβ2 of PKA.
- CD3/CD28 stimulation of wt and Cβ2 KO in T cells.
- Glucose sensitivity and consumption in T cells.
- Influence of pyruvate addition on CD3/CD28 stimulated Cβ2 ablated lymphocytes.

3 Materials and methods

All reagents and materials are listed in Appendix A.

3.1 Mice

The mice KO for Cβ2 on a C57BL/6:129SV/J genetic background, were kept at Department of Comparative Medicine at the University of Oslo according to required conditions. Cages from Green line IVC (Techniplast); GM 550 cage (391 x 199 x 160 mm) and GM 900 cage (395 x 346 x 213 mm) W x D x H with the amounts of one to five and five to ten mice were used. Each cage had a separated airflow of 0.05 m/s and a temperature of 23-25 °C, the humidity was 55-60 %. Water and food were available at all times. The rodent diet was soya based and consisted of 18 % Protein (Teklad Global 18 % Halan). The project was approved and registered by NARA.

3.2 Genotyping of mice

3.2.1 DNA isolation

Ear biopsies were mixed with a 4:1 mix of lysis buffer and Proteinase K (DNA Isolation Kit II Tissue, Roche, 03186229001) and incubated overnight at 56 °C in order to dissolve the tissues and digest proteins. The samples were vortexed, and to reduce risk of contamination, centrifuged at 300 x g for 30 s to remove moist in the lid. They were subsequently transferred to a 32 well cartridge designed for the MagNaPure machine (Roche), and isolation of DNA was done according to protocol provided by the manufacturer of the MagNa Pure LC DNA Isolation Kit (Roche, 03186229001). The DNA was stored at -20 °C until further analysis.

3.2.2 Genotyping of WT and Cβ2 KO mice by PCR

Ten µL of mouse DNA was mixed with 2.5 µL 5 x buffer without Magnesium Chloride ($MgCl_2$), 0.2 µL 25 mM deoxyribonucleotide Triphosphate (dNTPmix), 3 µL 25mM $MgCl_2$ (all provided by Expand High Fidelity PCR System, Roche), 0.5 µL mM of forward primer for identifying KO and WT (5`TGTAGGTCCTGCTGTATGCTTGTCTACCC), and reverse primers for KO (5` CTTGCTCCTTAGCCATTTCTTACTCCAGC) and wild type (wt)

(5`TATTTGCCTGTCTACATCATGCGTGTCAG) and mixed with 7.3 µL Dnase and Rnase free H_2O. Finally, 0.5 µL (2U/ µL) DNA polymerase (DyNAzyme, Thermo Scientific) was added to a total of 25 µL reaction volume.

The Veriti Thermal Cycler from Applied Biosystems was used for PCR with an initial denaturation step at 94 °C for 1.50 min, followed by 30 cycles comprising of denaturation at 94 °C for 0.50 min, annealing at 60 °C for 0.5 min and elongation at 68 °C for 3 min. A final elongation step at 72 °C for 2 min completed the program. The samples were kept at 4 °C until further analysis.

Agarose gels 1.5 % were stained with 10 µL SybrSafe (0.01 %) (Life Technologies) for visualization of DNA by UV-light. A standard 1 kB DNA ladder (Life Technologies, 1.0 µg/µL) was loaded together with a positive control. To make the PCR product denser, 5 µL of 6 x orange loading dye (2.5 g Ficoll, VWR, 0.025 g orange G, Sigma, 10 mL dH_2O) was added to each sample. Electrophoresis was conducted using an electrical field of 100 V for approximately 30 min (BIORAD POWER PAC 300).

3.2.1 Dissection of mouse lymph nodes, thymus and spleen

Mice were euthanized by cervical dislocation. Lymph nodes (axillary, brachial, inguinal and lumbar), thymus and spleen were dissected out aseptically (figure 10). The organs were placed in 10 mL sterile medium (Sigma).

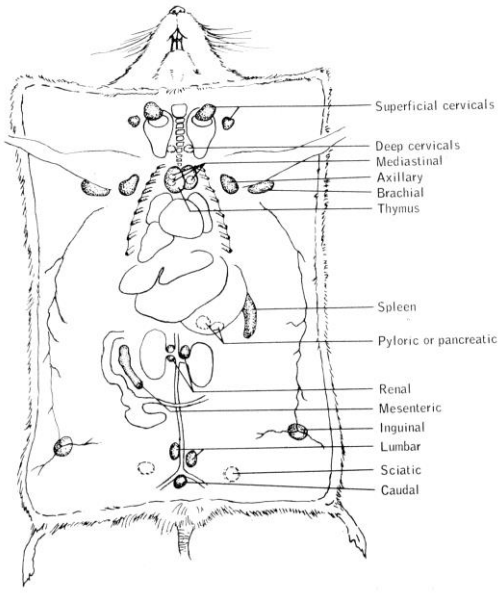

Figure 10. Diagram of Lymph nodes, spleen and thymus

After opening and fastening of the mouse, the axillary, brachial, inguinal and lumbar lymph nodes were first removed. Then the spleen was dissected out. Finally the thorax was opened to visualize the thymus, which was carefully detached and removed. All organs were placed in 10 mL sterile medium.

The organs were dissociated on a 70 µm cell strainer (Falcon) placed on a round petri dish (Costar) with 10 mL of ice cold isolation buffer (Sigma; 2 mM EDTA; 2 % Fetal Bovine Serum (FBS) (Sigma)) using the back of a syringe (BD Plastipak). The resulting cell solution was transferred to a 15 mL tube and centrifuged for 10 min at 300 x g at 4 °C. Supernatant was removed and the cells pellet resuspended in 5 mL cold isolation buffer. Red blood cells from spleen samples were lysed using 1 mL of Red Blood Cell Lysing buffer (Sigma), incubated for 5 min and added 9 mL of cold isolation buffer to stop the process. After centrifugation at 300 x g for 10 min at 4 °C, and removal of the supernatant, the cell pellets were resuspended in 5-10 mL of isolation buffer. Equal parts of cell suspension and Trypan Blue Stain 0.4 % (Life Technologies) were mixed and 10 µL transferred to counting chamber slides (Life Technologies) and counted on an automated cell counter Countess (Life Technologies). Cell pellets were either directly used in further analysis or washed twice in PBS (Sigma), centrifuged at 300 x g at 4 °C for 10 min, the supernatant removed, and transferred to Safe Lock Eppendorf tubes and stored at – 80 °C.

3.3 Western blotting/immunoblotting

3.3.1 Lysing of cells

Cell pellets from genotyped wt and KO mice were lysed in 100 µL lysis buffer (50 mM Tris pH 7,4, 100 mM NaCl, 5 mM EDTA, 50 mM NaF, 10 mM Napp, 1mM Na3VO4, 1 mM PMSF, 1% Triton) at 4 °C. The lysate was sonicated (1 s x 3 Amplitude 60 %) and incubated on ice for 30 min, vortexed and finally centrifuged at 16 000 x g speed for 15 min at 4 °C to remove debris. The supernatant was then transferred to new Eppendorf tubes and the protein concentration determined.

3.3.2 BCA Protein determination (Pierce)

BCA Protein assay is a colorimetric method for detection and quantification of total protein. The cell lysates were loaded on 96 well flat bottomed microtiter-plates (Greiner bio-one). Lysis buffer (5 µL) was added as blank and standard solutions with FBS (5 mg/mL, 2.5 mg/mL, 1.25 mg/mL, 0.625 mg/mL, 0.312 mg/mL) were loaded on the plate to determine concentrations. A 1:50 mix was made with BCA Reagent A and BCA Reagent B (Pierce BCA

Protein Assay, Thermo Scientific) and added to all wells. The plate was incubated at 37 °C for 30 min and then analyzed by a microplate reader (Fluostar OPTIMA, BMG LABTECH).

3.3.3 Western Blotting/immunoblotting

The lysates were adjusted to equal amount of protein and mixed with 3 x Sodium dodecyl sulphate (SDS) loading buffer (pH 8. 3) (187, 5 mM Tris HCl pH 6.8; 240 mM SDS; 30 % glycerol; 0.003 % bromphenol blue and 15 % 2-mercaptoethanol). The lysates were boiled for 5 min at 96 °C and then 30-40 µg of total protein was loaded on precast 12 well 10 % SDS-PAGE (Bio-Rad) with a 10 µL protein standard (Dual Color Standard, Bio Rad) as ladder. The proteins were separated by electrophoresis at 100-120 V for about 2 h (Bio Rad Power pack).

Afterwards, gels were was placed on top of a polyvinylidene fluoride membrane (PVDF) (Immobilion-P). A sponge and three Whatman paper sheets were placed under the gel (GE Healthcare UK Limited) (approximately 10 x 15 cm). It was then covered with three new Whatman paper sheets (all sheets were soaked in cold transfer buffer; 39 mM Tris-base, 48 mM glycine, 10 % methanol, pH 7.4), and a sponge. The “sandwich” was placed in a transfer tray (Bio Rad) and filled with cold buffer and an ice block for 45 min of 100 V. Afterwards, the PVDF membrane was blocked by drying overnight in room temperature.

After blocking overnight, the membrane was soaked in methanol (Emsure) and washed in 1 x TBST (10 mM Tris-Base; 0.1 % Tween 20; 150 mM Sodium Chloride, (NaCl); pH 7.5) before incubated with primary antibody (c-mono or anti RIa and RIIa in 10 mL TBST) for 1 h in room temperature on a Gyratory Rocker (Stuart Scientific). The blot was washed a total of six times, first time in TBST for 15 min, and again 5 times each of 10 min to remove excess antibodies.

The membranes were then incubated with secondary antibody for 1 h in room temperature and washed as previously described.

The blot was incubated for 5 min with a mix of equal amounts of solution A and B of Pierce Enhanced chemiluminescence kit (Thermo Scientific, 34080). Signal detection was performed using a SynGene apparatus with a camera that detects the chemiluminecense.
For western blot validation, a control antibody (GADPH, Sigma) was used. Equal amounts of Solution A and B of the SuperSignal West Dura Extended Duration Substrate kit (Thermo

Scientific, 34076) were used for detection. Procedures for washing and analysis were as previously described.

3.4 Protein Kinase A phosphotransferase assay

Ten µL of cell lysates (2 µg protein/ml) from lymph nodes, spleen and thymus were incubated with water (10 µL), cAMP (10 µL) or PKA-specific inhibitor (PKI) (10 µL) in 5 mL test tubes. To measure PKA-specific phosphotransferase activity, 30 µL Kemptide mix, with [γ-32P] ATP was added to each tube and incubated at 30 °C. After 9 min, the samples were spotted on a phosphocellulose paper (1. 5 x 3 cm) and dropped into a washing solution, a phosphoric acid bath (Sigma), to stop the reaction. The washing solution was changed and the filter papers were washed for 10 min. The washing step repeated two more times. Finally, the filter papers were washed for 10 min in 96 % ethanol; before the filter papers were air-dried on a Whatman 3M paper for 20-60 min. Kemptide assay mix (5 µL) was spotted in duplicate on the phosphocellulose papers to determine specific activity. The filter papers were then counted in a scintillation counter (TriCarb 3100TR, Perkin Elmer) in counting vials containing 3 mL scintillation cocktail (Ultima Gold F, Perkin Elmer).

3.5 Protocol for negative isolation of $CD4^+$ cells using Dynabeads

After counting, the lymph nodes, and spleen cells were centrifuged at 300 x g at 4 °C for 10 min and resuspended in ice cold isolation buffer (Sigma D8537; 2mM EDTA; 2% FBS, Sigma) and Antibody mix from the negative isolation of $CD4^+$ cell kit (Life Technologies,11415D). The volume of Antibody mix was adjusted according to number of cells, mixed well and incubated 20 min on ice. Subsequently the samples were added 10 mL of isolation buffer, mixed well and centrifuged at 350 x g at 4 °C for 8 min. The beads were resuspended and vortexed before they were washed according to manufacturer's protocol (Life Technologies). Cell pellets were resuspended in cold isolation buffer (4 mL) and beads (1 mL) and incubated for 15 min in room temperature at a roller mixer (Stuart Scientific). This ensures that antibody labelled bind to the beads surface, leaving $CD4^+$ cells in the solution (figure 11). The cells were then added 5 mL of isolation buffer and resuspended five times using a tip with a narrow opening, to avoid foam. The tubes were then placed on the

magnet for 2 min and the supernatant transferred to new tubes, containing only $CD4^+$ cells (Figure 11). The cells were counted and then centrifuged at 300 x g at 4 °C for 10 min, and resuspended in medium (Sigma) to a total of 1.5 x 10^6 cells/mL. The protocol for proliferation assay was then followed for further analysis.

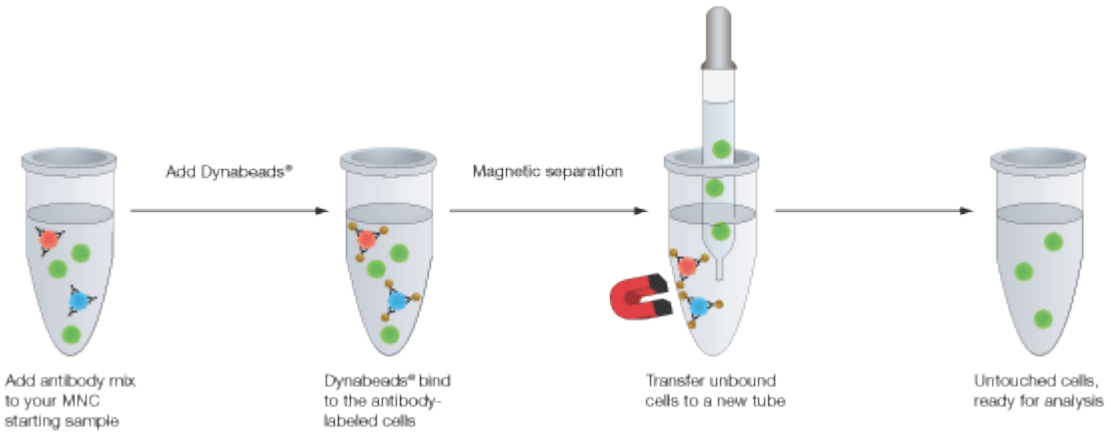

Figure 11. A representation of CD4+ isolation
The procedure for $CD4^+$ negative isolation using Dynabeads® Untouched TM Mouse $CD4^+$ Cells Kit (Life Technologies, 11415D). First; using Antibody mix, the Dynabeads attach to antibody labelled cells. Second; using a magnets, the untouched $CD4^+$ cells can be transferred to a new tube as the other cells remain (LifeTechnologies, 2014c).

3.6 Assay for anti CD3/CD28 induced T lymphocyte proliferation

After counting the cells, 50 µL of media with and without 1 % pyruvate (RPMI 1640, 1 % P/S, 1 % L-Glutamine, 1 % NEAA 10 % FBS, Sigma) of 1.5 x 10^5 cells were transferred to a 96 well plate (Costar) with round bottom. Dynabead Mouse T-Activator CD3/CD28 beads (Life Technologies) was vortexed, transferred to Eppendorf tubes, and washed according to protocol, provided by the manufacturer (Life Technologies). Incremental concentrations of beads were added to each sample in a 1.4 x 10^6 bead/mL (1:0.26, 1:0.53, 1:0.80, 1:1 or 1:1.3 bead: cell ratio). The beads activate T cells through CD3 and CD28 antibodies covalently bound to the bead surface which provide signals optimized for T cell activation and expansion (LifeTechnologies, 2014a) (figure 12). The plates were incubated for 44 - 48 h in 36.5 °C, with a 95 % humidity and 5 % CO_2, after 44 - 48 h 25 µL of [^{3}H]-Thymidine (PerkinElmer) (40 µCi/mL in 25 µL RPMI; 5% FBS, Sigma) was added to each well. Cells were then incubated for another 16 - 18 h before harvesting.

The [^{3}H]-Thymidine is incorporated into the DNA strands for each cell division, and the higher the proliferation rate, the more radioactivity will be incorporated. The [^{3}H]-Thymidine is a β-emitter with low radiation that allows for detection by the scintillation counter during harvesting (Härkönen, 2001).

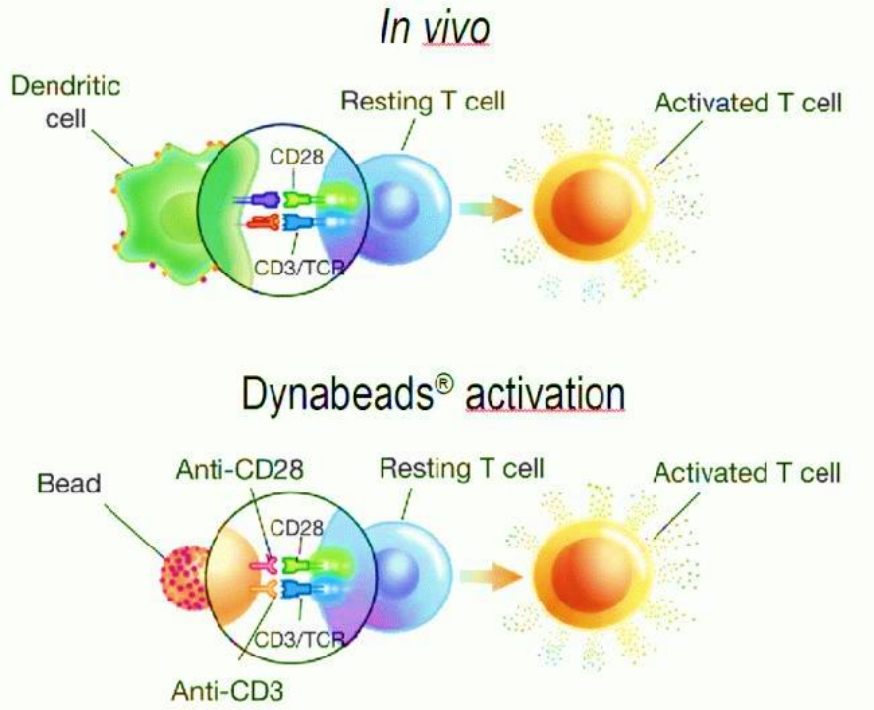

Figure 12. Representation of T cell activation
Above: Representation of *In vivo* T cell activation by CD3/CD28 activation signals. Below: Representation of T cell activation with CD3/CD28 bound to a 3 D bead (LifeTechnologies, 2014b).

3.6.1 Harvesting the cells

Cells were harvested to a 96 well filter plate (PerkinElmer) using a cell harvester (Packard Harvester) and placed for drying at 50 °C for 1-2 h. Particles bigger than 1.5 µm are collected by the filter membrane. After sealing the bottom of the filter plate, 25 µL of scintillation liquid (PerkinElmer) was added to each well. The filter plate was then sealed on top and incubated for 20 min in room temperature before being placed in a scintillation counter (Packard).

3.7 Glucose assay

Pooled samples from wt and KO mice were adjusted to a concentration of 1.5 x 10^6 cells/mL. The samples were centrifuged at 300 x g at 4 °C for 10 min, supernatant removed, resuspended in 1 mL of glucose free media (Gibco), mixed with prewashed beads and then added to the wells in a round bottomed plate (Costar).

Afterwards, media with incremental glucose concentrations were added to each well, leaving the end concentration in the wells to 0, 1, 5, 15 and 25 mM respectively. The glucose concentrations were verified by using a glucose test apparatus (ACCU-CHEK Aviva) (Roche) with test strips (Roche). A reliability test of the apparatus and the concentrations in the tubes used in the experiment was also performed. According to the manufacturer, the glucose apparatus does not detect values below 0.6 mM or above 33.3 mM. Therefore, in results, table 1 and table 2; "Lo" appears for the media concentration devoid glucose and "HI" appears for a glucose concentration at 50 mM.

The plates were incubated for 24 - 48 h at 36.5 °C, with a 95 % humidity and 5 % CO_2, after 24 - 48 h 25 µL [3H]-Thymidine (PerkinElmer) (40 µCi/mL in 25 mL of Gibco; 1 % P/S, Sigma) and incremental glucose concentrations of 0, 1, 5, 15 and 25 mM respectively. Cells were then incubated for another 16 - 18 h before harvesting.

3.7.1 Filtration of Fetal Bovine Serum for glucose free media

FBS (Sigma) was filtrated and sterilized to remove any contaminants larger than 0.2 µm. A big glass container with a magnet was filled with dH_2O (3 L) and PBS (Sigma. 1 tbl/200 mL). The Slide-A-Lyzer Cassette (Thermo Scientific) was removed from its pouch and rehydrated in the buffer solution for two min. Without blotting the membrane the cassette was gently dried and filled with FBS (Sigma) using a syringe (BD Plastipak TM; Sterican) containing the sample, leaving very little air inside. The cassette was fastened to a buoy and was rotating overnight at 4 °C. To sterilize the sample, a syringe and a sterile filter (Life Sciences) (0.2 µm) was used to withdrawing the sample.

3.8 Statistical analysis and evaluation of Western blot

For Kinase Assay, negative isolation of $CD4^+$ cells, proliferation assay and glucose assay, GraphPad Prism version 6.04 and Statistical Analysis for the Social Sciences version 22 was used for creation of bars, graphs and running statistical analysis. Data are presented as means ± Standard Deviation (SD). Independent sample T test was used to investigate differences between wt and Cβ2 KO mice. Glucose consumption in T cells over time was tested with paired sample t-test for analysis from triplicate measurements. These data were presented with Statistical Error of the Mean (SEM). Because few mice and triplicate tests creates a high uncertainty, one takes into consideration that mice are genetically inbred, which means that the mice are close to genetically equal and that few mice can set indications for a bigger population. A p-value of ≤ 0.05 is indicated by * considered statistically significant. Further, a p-value of ≤ 0.005 is indicated by **.

For RIα and RIIα WB analysis, GeneTools and GeneSnap from SynGene (VWR) were used for analysis and quantification.

4 Results

4.1 Cβ2 ablation proved by PCR and Western blot

To ensure the genotype of the mice, ear biopsies were analysed with PCR using specific primers (see Material and methods and attached booklet from genOway). Figure 13, depicts an example of performed PCR. Lanes 2 and 6 show PCR products of 557 and 319 bp, respectively, whereas lanes 3 and 5 represent a specific DNA product of 557 bp and lane 4 DNA of 319 bp. This means that the samples came from heterozygote (wt/KO) mice (lanes 2 and 6), homozygote Cβ2 KO mice (lane 3 and 5) and wt mouse (lane 4). The Cβ2 KO mice were used for further breeding and experiments.

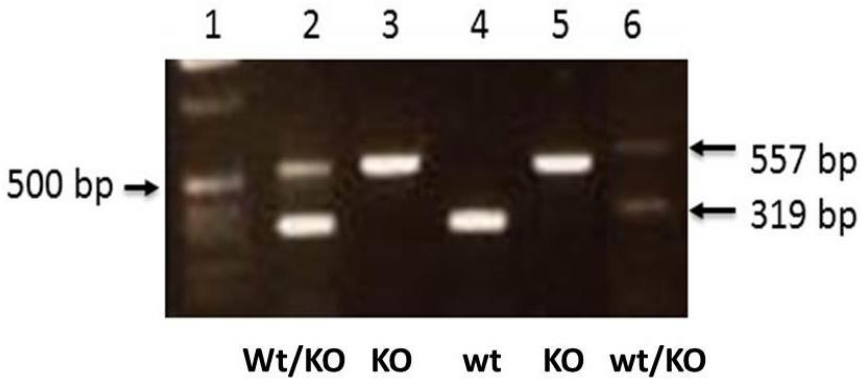

Figure 13. Genomic characterization of Cβ2 KO and wt mice
PCR products of ear biopsies from homozygote wt, Cβ2 KO and heterozygote (wt/KO) mice. The wt and KO alleles runs at 319 and 557 kb respectively. 1 Kb ladder was added to lane 1. Lane 2 and 6 represent wt/KO, while lane 3 and 5 represent KO and lane 4 represent wt.

As mentioned, Cβ2 is expressed in immune cells of the spleen (Funderud, Henanger et al. 2006). Using immunoblotting and a pan-C monoclonal antibody spleen was initially tested for the expression of Cβ2. This demonstrated that wt spleen cells express anti-C reactive proteins of 40 and 47 kDa (lanes 4-6, figure 14 A) and that spleen cells from Cβ2 KO lack immunoreactive proteins running at 47 kDa (lanes 1-3). The Skålhegg group has also previously shown that Cβ2 is expressed in the immune cells T, B and NK cells, which resides in the thymus and lymph nodes as well as the spleen (Funderud, Henanger et al. 2006). Hence, we tested the expression of Cβ2 in cells isolated from wt and Cβ2 KO cells of these tissues. Figure 14 B shows that Cβ2 immunoreactive protein of 47 kDa is ablated in cells from Cβ2 KO cells from lymph node (lane 2), spleen (lane 4) and thymus (lane 6).

A.

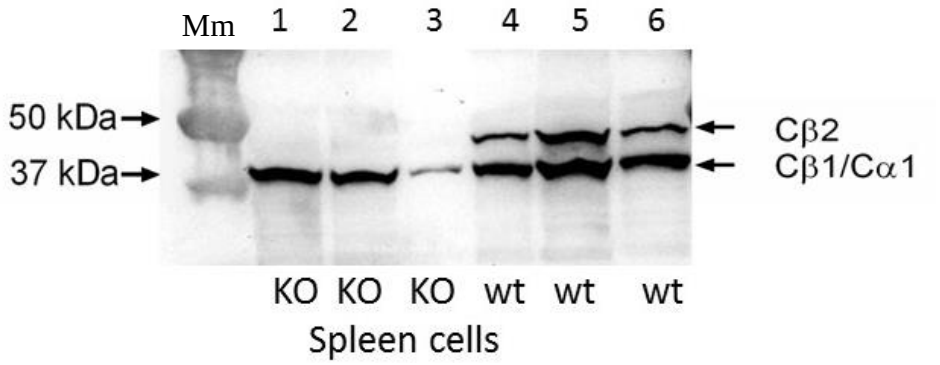

B.

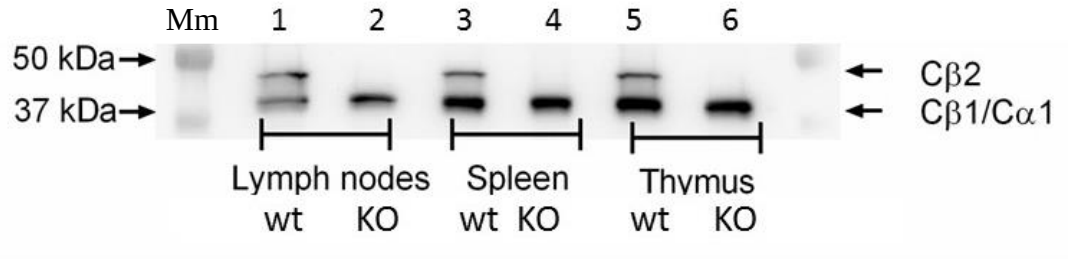

Figure 14. WB analysis of PKA C subunit expression in Cβ2 KO and wt mice
WB analysis of C subunit expression in splenocytes isolated from three KO (lanes 1-3) and wt mice (lanes 4-6) (A). WB analysis of C subunit expression in cells isolated from lymph node, spleen and thymus from three KO and wt mice (B). Lanes 1, 3 and 5 represent wt while lanes 2, 4 and 6 represent KO mice. In panel A and B cell extracts (15-25 µg protein/lane) were separated by 10 % SDS-PAGE and transferred to PVDF membranes. Immunoreactive proteins were recognized with anti-C (mouse monoclonal, 1:100 dilutions) and visualized with a secondary Horseradish Peroxidase (HRP)-conjugated anti-IgG antibody.

4.2 Comparison of PKA C subunit activity in immune tissues from Cβ2 wt and KO mice

To determine total PKA activity after Cβ2 ablation, thymocytes, lymph node cells and splenocytes were isolated and cell extracts monitored for cAMP-inducible PKA activity. Previous research has shown that there is a reduction in PKA activity in lymph node, spleen and thymus lysates in Cβ KO mice (A. Funderud et al., 2006; Orstavik et al., 2005). The PKA-specific kinase activity was reduced by 52 %, 39 % and 37 % in cell lysates made from Cβ2 KO lymph node, spleen and thymus cells, respectively, compared to wt (figure 15).

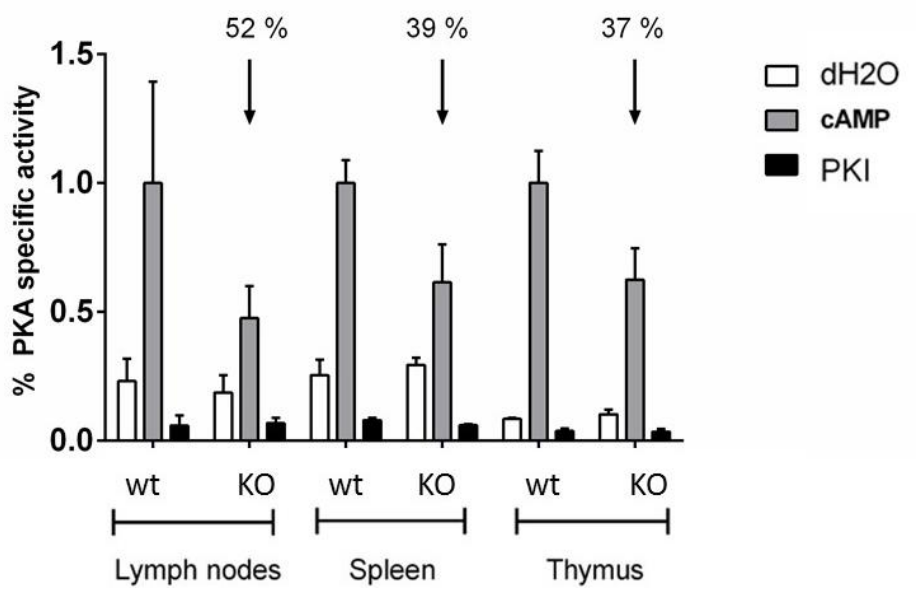

Figure 15. Comparison of PKA-specific phosphotransferase activity in lymph node, spleen and thymus cell lysates from Cβ2 KO and wt mice

The activity was measured as incorporation of ^{32}P in the PKA-specific substrate Kemptide in the presence (cAMP) and absence (dH_2O) of cAMP and in the presence of the PKA-specific inhibitor (PKI). Activity in the extracts from Cβ2 KO mice were given relative to the activity in the lysates from wt mice, which were set to 1. Bars represent mean activity from four experiments ± S.D. Arrows indicate percentage reductions in activity, with a 37 - 52 % decrease in activity of lysates from KO mice.

4.3 Comparison of PKA RIα and RIIα in immune tissues from wt and Cβ2 KO mice

Based on PKA C subunit activity and the fact that subunits RIα and RIIα of PKA are expressed in T and B cells, 80 % and 10-20 % respectively (Orstavik et al., 2005), we tested for RIα and RIIα expression in wt and Cβ2 KO mice cells from the lymph node, spleen and thymus. Figure 16 panels A and C show the level of immune reactive RIα and RIIα in lymph nodes, spleen and thymus, and figure 16 B and D show the quantification of protein expression when normalized to Glyceraldehyde 3-poshphate dehydrogenase (GADPH). There were no significant differences in RIα or RIIα expression from wt and KO mice amongst the tissues, which implies an R to C ratio above 1 in Cβ2 ablated lymphocytes. This could further indicate that PKA holoenzyme is less sensitive to cAMP in Cβ2 ablated cells.

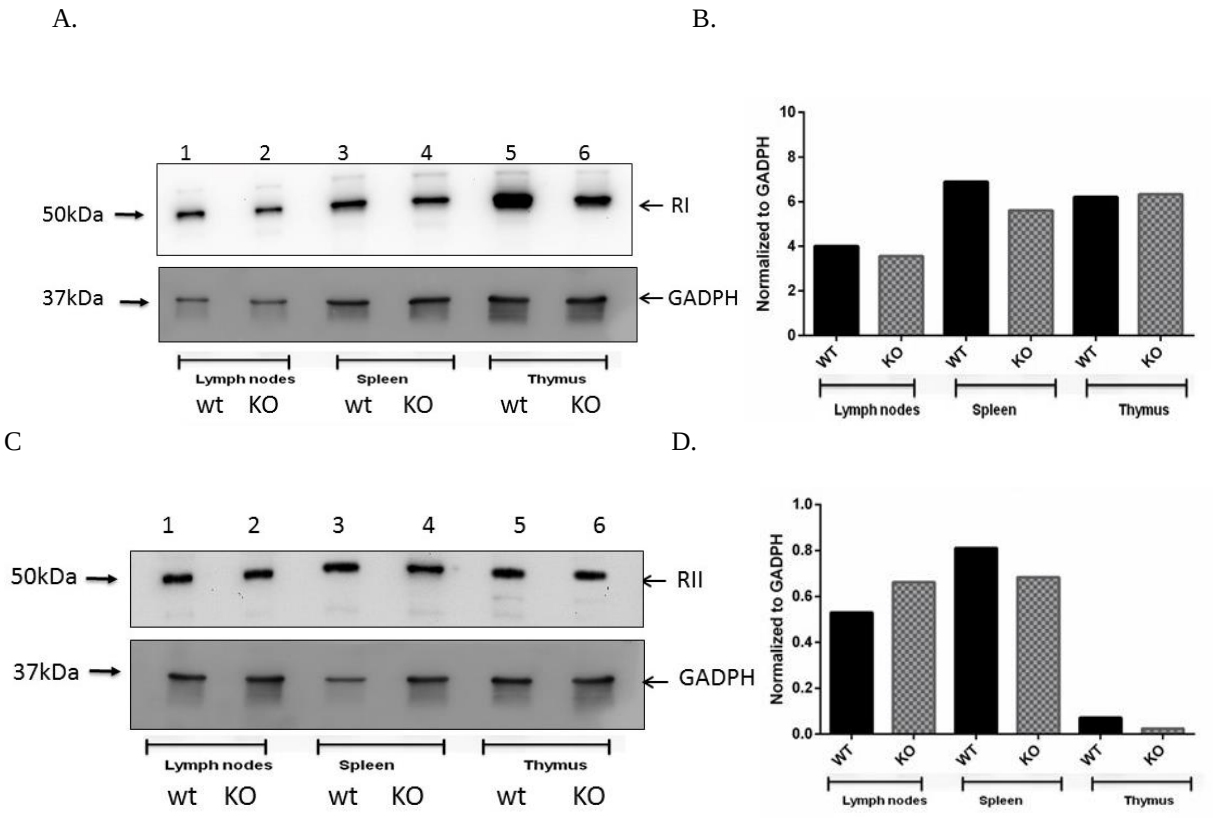

Figure 16. Identification and quantification of RIα and RIIα expression from lymph node, spleen and thymus cell lysates (30 µg) from three Cβ2 KO and wt mice
Proteins were separated by 10 % SDS-PAGE followed by transfer to PVDF membranes. Identical blots were incubated with anti-human RI, (mouse monoclonal, 1:100 dilution) (A) anti- human RII (mouse monoclonal, 1:100 dilution) (C) or anti-GADPH (rabbit polyclonal, 1:100 dilution) (A and C). Secondary HRP-conjugated anti-IgG antibody was used for detection. Lanes 1, 3 and 5 represent wt mice and lanes 2, 4 and 6 represent KO mice. Arrows to the left indicate molecular size, arrows to the right indicate protein identity (RIα, RIIα and GADPH). Analysis in GeneSnap provided values for quantification of WB by using GADPH as loading control. Values were normalized to GADPH (B and D).

4.4 Anti-CD3/CD28 induced proliferation in lymph node and spleen cells

As mentioned in the introduction, a rise in endogenous cAMP inhibits T and B cell proliferation and clonal expansion, as well as NK cell cytotoxicity (Torgersen, Vang, Abrahamsen, Yaqub, & Tasken, 2002). To determine if the decreased PKA activity observed in Cβ2 KO immune tissues influence T cell proliferation, we use anti-CD3/CD28 antibodies attached to magnetic beads. These beads are known to mimic a situation of APC-dependent activation of T cells. Lymph node, spleen and thymus cells from Cβ2 KO and wt mice were stimulated with different ratio of anti-CD3/CD28 coated beads to find the optimal ratio for maximal proliferation. Cells from both lymph node and spleen show optimal proliferation between 8 x 10^4 and 2 x 10^7 bead/mL (panels A and B). A repeatedly observed low proliferation rate in thymocytes with values close to non-stimulated cells (data not shown), excluded the thymocytes from future inclusion in this thesis.

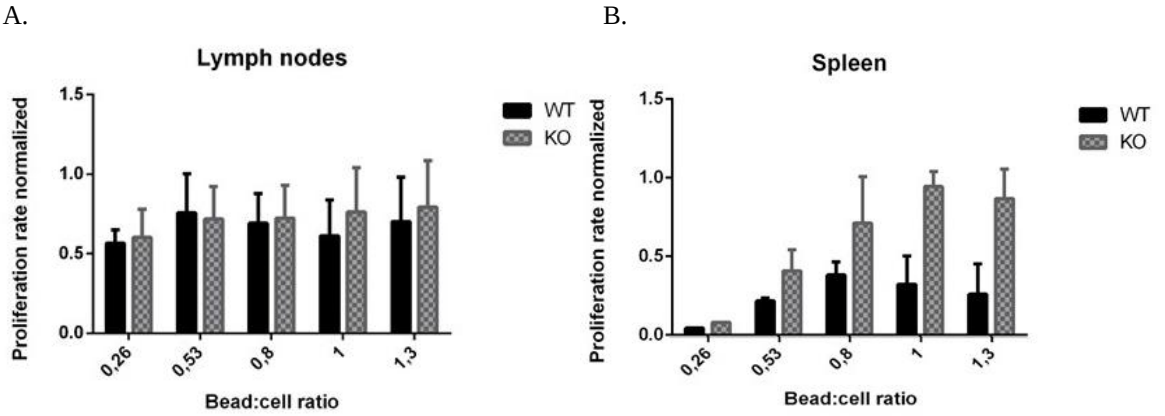

Figure 17. Dose-dependent anti-CD3/CD28 induced lymphocyte and splenocyte proliferation
Pooled cells of 1.5 x 10^6 cells/mL, isolated from Cβ2 KO and wt mice, were stimulated with anti-CD3/CD28 coated beads at a ratio of 1:0.26, 1:0.53, 1:0.8, 1:1 or 1:1.3, for 72 h. [^{3}H]-thymidine (40 µCi/mL) was added the last 18 h of incubation before harvesting. Figures A and B represent normalized proliferation rates in lymphocytes, and splenocytes from eight and six KO and wt mice, respectively. The highest proliferation rate was set to 1 and other results set relative to 1. Bars in A and B represent the mean from triplicate values ± S.D.

4.5 Induced CD3/CD28 cell proliferation influences CD4+ Cβ2 ablation in splenocytes, but not in lymph node cells

Experiments depicted in figures 17 A and B demonstrated dose-dependent CD3/CD28 induced proliferation of a mixed cell population. Hence, our results may have been influenced by the presence and action of a number of non-T cells, such as NK cells, monocytes, macrophages and dendritic cells. To more precisely define the effect of Cβ2 ablation on T cell proliferation we isolated $CD4^+$ T cells as described in Material and methods. We used 1.4 x 10^6 bead/mL that demonstrated no apparent difference in anti-CD3/CD28 induced proliferation between wt and Cβ2 KO $CD4^+$ lymph node cells (panel A). However, a significantly higher proliferation rate was observed in $CD4^+$ spleen cells from Cβ2 KO compared to wt (p-value 0.03, panel B). The significant increase in proliferation in $CD4^+$ spleen cells could imply that Cβ2 could influence $CD4^+$ cells in splenocytes or that other mechanisms in the spleen are at work.

A. B.

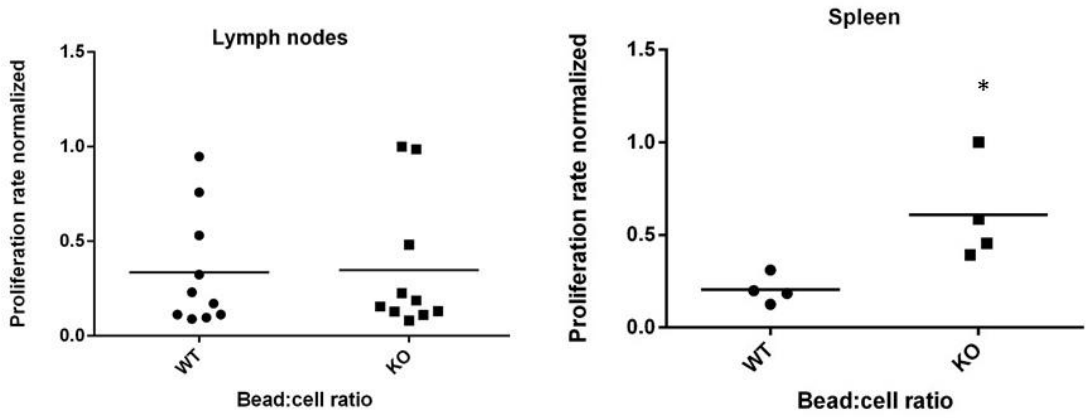

Figure 18. Cβ2 ablation influence anti-CD3/CD28 specific $CD4^+$ splenocyte but not lymphocyte proliferation
Cβ2 KO, wt and wt $CD4^+$ cells (1.5 x 10^6 cells/mL) were stimulated with anti-CD3/CD28 of 1.4 x 10^6 beads/mL for 72 h. [^{3}H]-thymidine (40 µCi/mL) was added the last 18 h of incubation before harvesting. A Present normalized lymphocyte proliferation rate from 10 KO and wt mice from two experiments. B Present normalized splenocyte proliferation rate from four KO and wt mice. A significantly higher proliferation rate was found in splenocytes for Cβ2 KO compared to wt (p-value < 0.03 (C) and p-value < 0.003(D)). The highest proliferation rate was set to 1 and other results set relative to 1. Dots represent the mean from triplicate and sixtuplicate values ± S.D (A and C).

4.6 Glucose consumption and proliferation in lymph node and spleen cells.

4.6.1 Reliability test of glucose apparatus and confirmation of glucose concentrations used in glucose assay

As immune cell proliferation requires increased uptake of glucose and PKA inhibits immune cell proliferation as well glucose uptake and metabolism in the liver and muscle, we investigated if glucose uptake by Cβ2 KO immune cells and $CD4^+$ T cells were altered compared to wt cells.

First, an equilibration test of the glucose test apparatus was performed to assure that theoretical glucose concentrations were comparable to glucose concentrations used in the assays (panels A and B, table 1 and 2). The glucose dependence and consumption was studied in proliferating T cells stimulated through their CD3/CD28 cell surface markers. Panels A and B depicts concentrations used in the glucose assays ± S.D. Data indicate that the measured values (0 - 30 mM and 0 - 25 mM) are almost according to theoretical values.

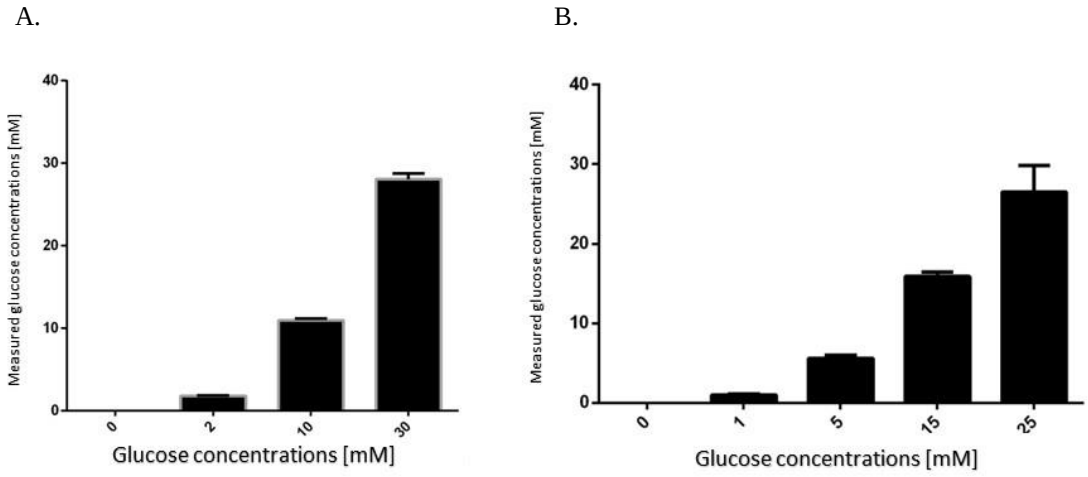

Figure 19. Actual versus measured glucose concentrations
Concentrations of glucose were made in order to provide cells with incremental glucose concentrations (0-25 mM) provided by the glucose test apparatus (ACCU-CHEK Aviva). It ascertains that the apparatus was equilibrated correctly and verifies the concentrations used in the research. Figure A presents concentrations that were diluted 50 % in each sample when added. Figure B presents concentrations that contained [^{3}H] thymidine (40 µCi/mL). Bars in panel A and B represent the mean from measured triplicate values ± S.D.

Table 1 and 2 present theoretical values of incremental concentrations of glucose, the mean from measured values and the percentage deviation from theoretical values to measured concentrations.

Table 1: Theoretical versus measured concentrations of glucose. Deviations from theoretical values are presented as percentage.

Glucose concentrations [mM]						
Concentration (theoretical values)	0	2	10	30	50	
Measured average concentration	LO*	1.8	11.0	28.1	HI*	
Deviation (%)	-	10 %	10 %	6.3 %	-	

*"LO" < 0.6 mM, **"HI" > 33.3 mM.

Table 2: Theoretical versus measured concentrations of glucose. Deviations from theoretical values are presented as percentage.

Glucose concentrations with [3H]-thymidine [mM]							
Concentration (theoretical values)	0	1	5	15	25		
Measured average concentration	LO*	1.0	5.6	15.9	26.5		
Deviation (%)	-	-	12.0 %	6.0%	6.0 %		

*"LO" < 0.6 mM.

4.6.2 Glucose-dependent anti-CD3/CD28 induced proliferation of Cβ2 KO and wt lymph node and spleen cells

To investigate the dependence of the glucose concentration on immune cell proliferation, lymph node and spleen cells from Cβ2 KO and wt mice were stimulated with anti-CD3/CD28 coated beads in media with incremental concentrations of glucose (0 - 25 mM). This demonstrated that glucose concentrations below 1 mM are incompatible with cell proliferation (panels A and B). It was no apparent difference in the rate of proliferation if the cells were grown in the presence of 1 or 5 mM glucose in lymphocytes after 72 h. Further, there was no observed difference in glucose dependence between wt and Cβ2 KO cells.

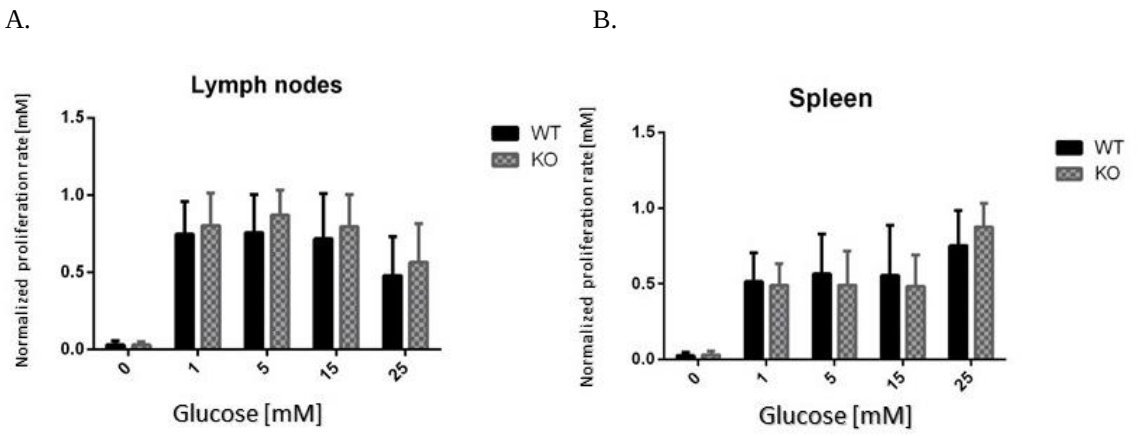

Figure 20. Glucose-dependent anti-CD3/CD28 induced proliferation of Cβ2 KO and wt lymphocytes and splenocytes
Pooled cells from six Cβ2 KO and six wt mice with 1.5 x 10^6 cells/mL were stimulated with anti-CD3/CD28 of 1.4 x 10^6 beads/mL for 72 h in the presence of incremental concentrations of glucose (0-25 mM). [^{3}H] thymidine (40 µCi/mL) was added the last 18 h of incubation before harvesting. Normalized proliferation rate for lymphocytes and splenocytes in media with glucose concentrations of 0, 1, 5, 15 and 25 mM are presented (A and B). Highest proliferation rate was set to 1 and other results given relative to 1. Bars in panel A and B represent the mean from triplicate values ± S.D.

4.6.3 Time-dependent glucose consumption by lymph node cells stimulated with anti-CD3/CD28

Next, the glucose consumption of CD3/CD28 stimulated lymph node cells at various time points 0, 24 and 72 h was monitored. Only a significant increase in glucose consumption for lymph node cells grown in 5 mM, panel A, in the time interval 0 to 24 h (p-value < 0.004) was observed. There appeared to be no difference in glucose consumption between Cβ2 KO and wt mice, at any fixed concentrations of glucose (5, 15, 25 mM) or at any time of measurements (0, 24 and 72 h).

A.

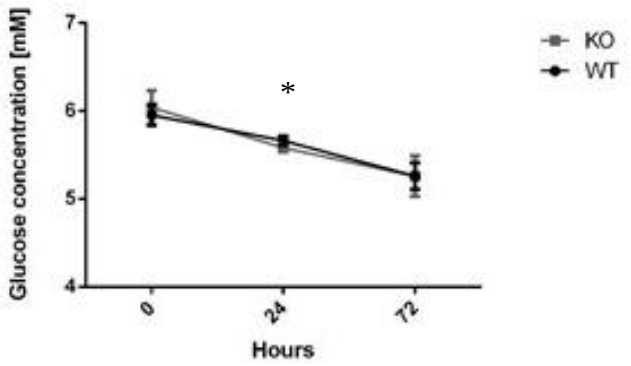

B.

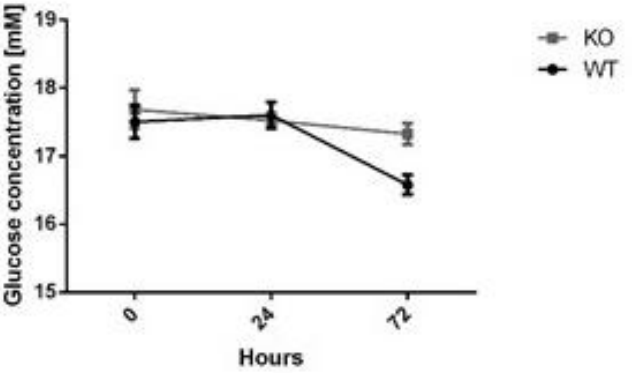

C.

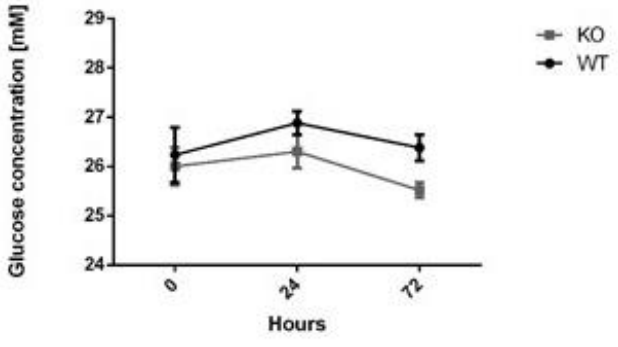

Figure 21. Time-dependent glucose consumption in lymph node cells
Lymph node cells (1.5 x 10^6 cells/mL) were isolated from six Cβ2 KO and six wt mice and stimulated with anti-CD3/CD28 coated beads (1.4 x 10^6 beads/mL) in the presence of 5 (A), 15 (B) and 25 mM glucose (C). Proliferation was measured after 24 and 72 h. Cells harvested after 24 h were added [^{3}H] thymidine (40 µCi/mL) at 0 h, while cells harvested after 72 h were added [^{3}H]-thymidine (40 µCi/mL) the last 18 h of incubation. Figures A show a significant increase in glucose consumption for both Cβ2 KO and wt from 0 to 24 h (p-value < 0.004). Figures B and C show glucose consumption in a concentration of 15 and 25 mM, over time. Dots represent the mean from triplicate values ± SEM.

4.6.4 Time-dependent glucose consumption by splenocytes stimulated with anti-CD3/CD28

Then, glucose consumption of CD3/CD28 stimulated splenocytes at 0, 24 and 72 h was monitored. There was no difference in glucose consumption (panels A - C), and no difference in consumption between Cβ2 KO and wt mice, at any fixed concentrations of glucose (5, 15, 25 mM) or at any time of measurements (0, 24 and 72 h).

A.

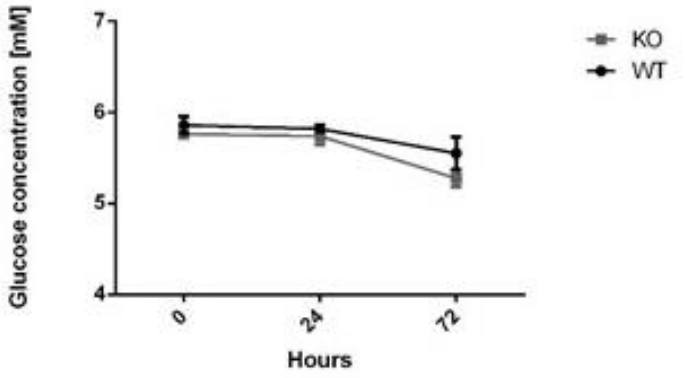

B.

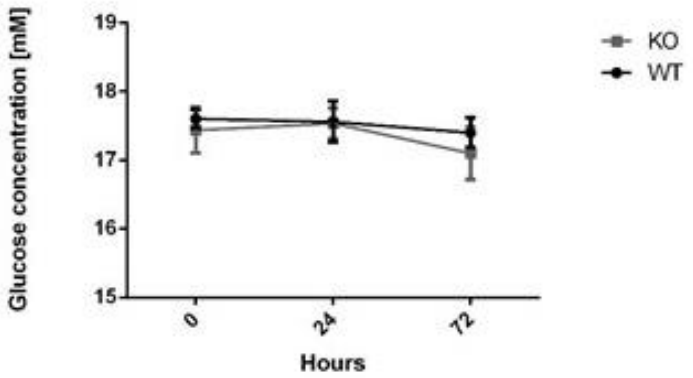

C.

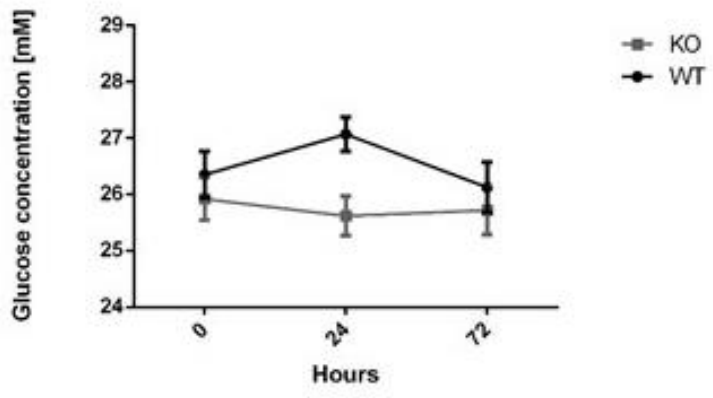

Figure 22. Time-dependent glucose consumption in spleen cells
Spleen cells from six Cβ2 KO and six wt mice and stimulated (1.5 x 10^6 cells/mL) with anti-CD3/CD28 coated beads (1.4 x 10^6 beads/mL) in the presence of 5 (A), 15 (B) and 25 mM glucose (C). Proliferation was measured after 24 and 72 h. Cells harvested after 24 h were added [^{3}H]-thymidine (40 µCi/mL) at 0 h, while cells harvested after 72 h were added [^{3}H]-thymidine (40 µCi/mL) the last 18 h of incubation. No significant increase was detected. Figures A, B and C show glucose consumption in a concentration of 5, 15 and 25 mM, over time. Dots represent the mean from triplicate values ± SEM.

4.6.5 Anti-CD3/CD28 induced proliferation at different glucose concentrations in lymph node and spleen cells

We next measured anti-CD3/CD28-dependent cell proliferation of lymph node cells (panels A - C) and splenocytes (panels D - F) at concentration of glucose (0-25 mM). This revealed no proliferation at time 0 and high levels of proliferation at 72 h at glucose concentrations between 1 and 25 mM. It appeared that proliferation was optimal at 1-15 mM glucose and no apparent differences were observed between Cβ2 KO and wt mice when cells are given incremental concentrations of glucose.

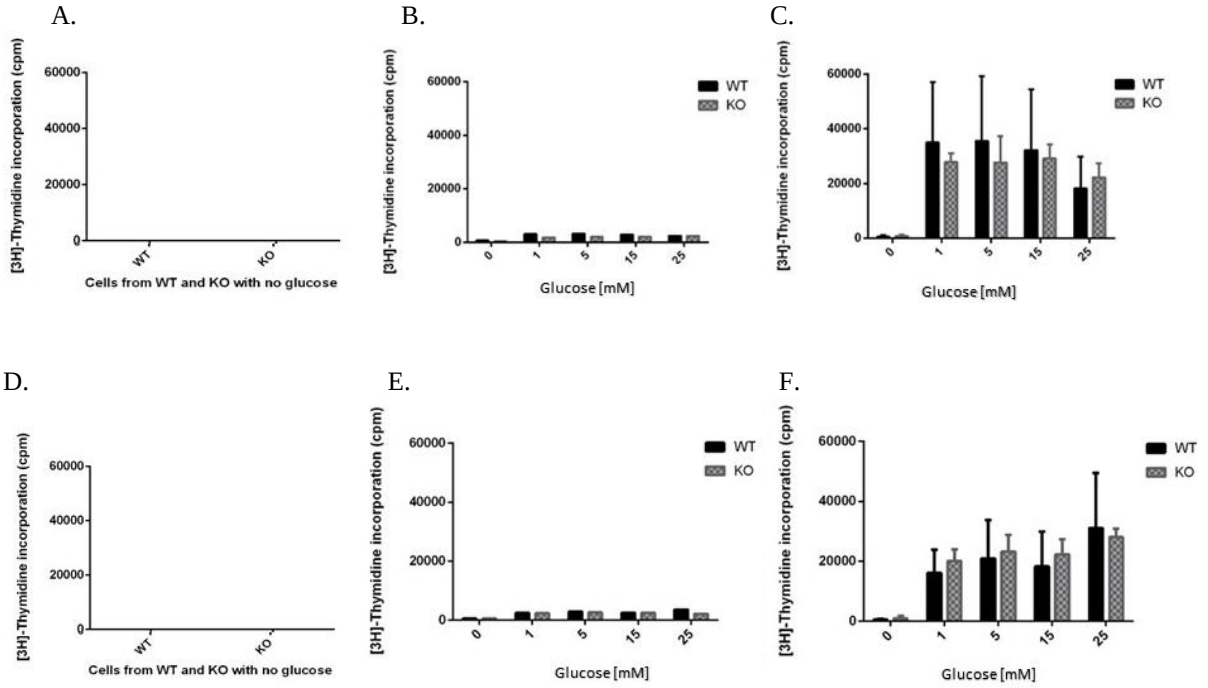

Figure 23. Anti-CD3/CD28 induced lymphocyte and splenocyte proliferation at incremental glucose concentrations (0-25 mM) Cells from six Cβ2 KO and wt mice (1.5 x 10^6 cells/mL) were stimulated with anti-CD3/CD28 (14 x 10^6 beads/mL) for 72 h. [^{3}H]-thymidine (40 µCi/mL) was added the last 18 h of incubation before harvesting. Proliferation (cpm) of cells in media without glucose at 0 hours (A and D). Incremental concentrations of glucose (0-25 mM) at 24 h (B and E) and 72 h (C and F). Bars represent the mean from triplicate values ± SD.

4.7 Pyruvate induces proliferation rate in lymph node and spleen cells

As explained in the introduction, pyruvate is a metabolic intermediate from glycolysis, where one molecule of glucose is converted into two molecules of pyruvate. Based on the availability of O_2, it may be converted to acetyl-CoA and enter the TCA cycle or converted to lactate by lactate dehydrogenase. As pyruvate is a down-stream product of glucose in the glycolysis it has been suggested as a potent and"fast" source of energy for proliferating cells. The fact that PKA is involved in regulating glycolysis in the liver and muscle cells, made it interesting to investigate if knockout of Cβ2 of PKA would influence pyruvate consumption in proliferating T cells.

CD3/CD28 stimulated wt and Cβ2 KO cells from both lymph nodes and spleen proliferate at a significantly higher rate than the same cells ablated for Cβ2 (p-value < 0.005, panel A; p-value < 0.001, panel B). The same pattern was observed when cells were grown in media with pyruvate. It should also be noted that cell proliferation by wt cells were more influenced by pyruvate addition than Cβ2 KO, and cells from wt proliferated at a significantly higher rate than Cβ2 KO cells when cells were in medium with pyruvate (p-value < 0.005, panel A; p-value < 0.007, panel B).

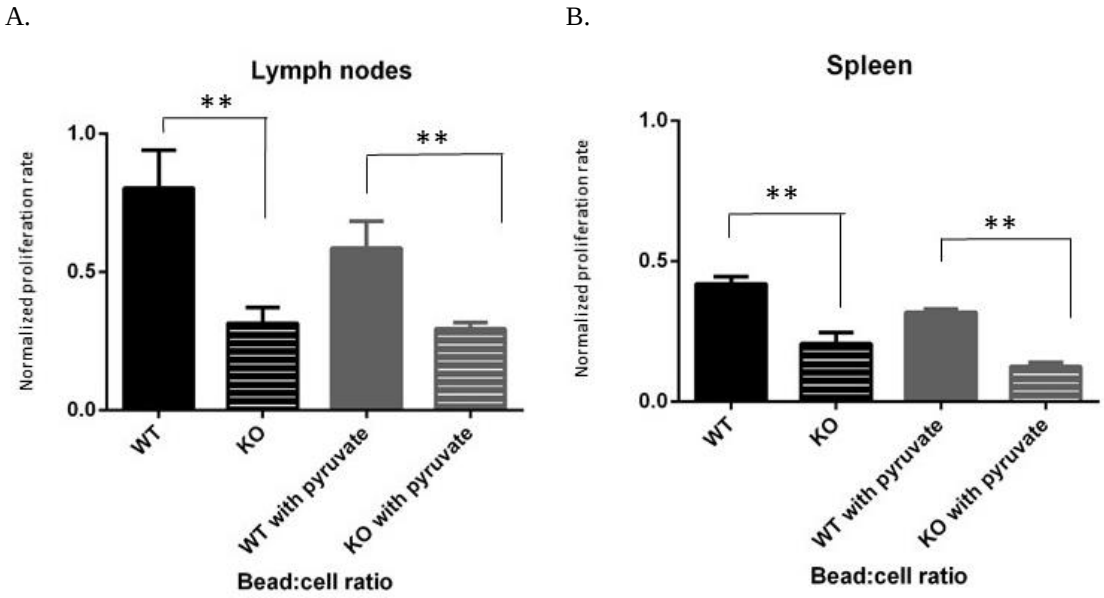

Figure 24. Anti-CD3/CD28 induced normalized proliferation rate in lymphocytes and splenocytes
Three Cβ2 KO and wt mice with cells from lymphocytes and splenocytes of 1.5 x 10^6 cells/mL were stimulated with anti-CD3/CD28 of 1.4 x 10^6 beads/mL for 72 h. [^{3}H]-thymidine (40 µCi/mL) was added the last 18 h of incubation before harvesting. A significantly higher proliferation rate for lymphocytes and splenocytes from wt

compared to KO (p-value < 0.005 (A); p-value < 0.001 (B)) were found. For cells in media with pyruvate, there was a significantly higher proliferation rate for lymphocytes and splenocytes from wt compared to KO (p-value < 0.005 (A); p-value < 0.007 (B)). The highest proliferation rate was set to 1 and other results set relative to 1. Bars represent the mean from triplicate values ± S.D.

5 Discussion

In an approach to understand the role and function of Cβ2 in regulating immune cell function, we studied T cell proliferation and glucose consumption in wild type mouse T cells and compared the results to T cells ablated for the catalytic subunit Cβ2 of Protein Kinase A.

5.1 The mouse as a model to study molecular function

5.1.1 Mice as models

When performing experimental research on whole organisms, animal mice models are widely used and well-established as a method. Animal models can help us understand how a single gene or clusters of genes can influence, numerous biochemical and physiological processes in various biological systems, including how nutrition and metabolism of nutrients such as glucose and amino acids are required for optimal and correct immune responses. Furthermore, the method may allow us to follow genetic disease-processes over time (even generations) (S. Feil, Valtcheva, & Feil, 2009). Mouse models are often used because of the similarities in the mouse genome with other mammals including humans. Results from mouse studies have been transferred to humans on a number of occasions with success. Despite this it´s important to be aware of important differences (Mestas & Hughes, 2004). For example most mice lines used in research are genetically inbred, which means that they show a high degree of genetic identity. Hence, laboratory mice do normally resemble wild type mice if the laboratory mice are not bred as F1 generations which represent the first filial generation of offspring of distinctly different parental types (Runge&Patterson, 2006). The results in this thesis are obtained from mice which are born with a constitutive KO on an inbred strain made by mixing C57BL/6J and 129Sv/Pas mice. The mice used in the present study were generated to carry a genetically null mutation of the Cβ2 subunit of PKA (in Appendix B is a final report on the Cβ2 KO phenotype by Genoway).

5.1.2 INDUCEBLE KO APPROACH

As explained in the introduction, the gene we wanted to investigate was removed by targeted mutation of exon 1-2 in the PRKACB gene. Exon 1-2 is used by the PRKACB gene to introduce a unique N-terminal end to Cβ2. Targeting this exon was done to produce mice that

were born without the Cβ2 protein (Moen, Eriksen and Skålhegg, unpublished). According to Feil and coworkers (2009) and others, the technique on Inducible Cre Mice, by Cre lox recombination by tamoxifen-induce Cre recombinase activity is the most successful CreERversion per 2009 (R. Feil, Wagner, Metzger, & Chambon, 1997; S. Feil et al., 2009; Indra et al., 1999). In many ways, it is similar to the KO approach used to delete the PRKACB exon 1-2. It uses a conditional gene targeting site-specific recombinase Cre (*c*yclization *re*combination), which catalyzes two floxed loxP DNA recognition sites. However, the *in vivo* Inducibility method ligand-dependent chimeric Cre recombinases, a so-called CreER recombinase, is developed because of activation of the synthetic estrogen receptor ligand 4-hydroxytamoxifen (OHT) (R. Feil et al., 1996; R. Feil et al., 1997; Metzger, Clifford, Chiba, & Chambon, 1995; Zhang et al., 1996) Cre is in this case fused with a mutated hormone-binding domain by the estrogen receptor. Cre ER is inactive and can be activated both spatially and temporally by tamoxifen, as tamoxifen metabolizes to OHT (or by use of tetracycline as inducer (St-Onge, Furth, & Gruss, 1996). This ability makes it possible to control floxed chromosomal DNA combined with tissue-specific expression of a CreER recombinase. As this is an instrument for controlling gene activity in space, time and tissue, it can provide information regarding the gene product at a certain developmental stage (Branda & Dymecki, 2004; R. Feil, 2007).

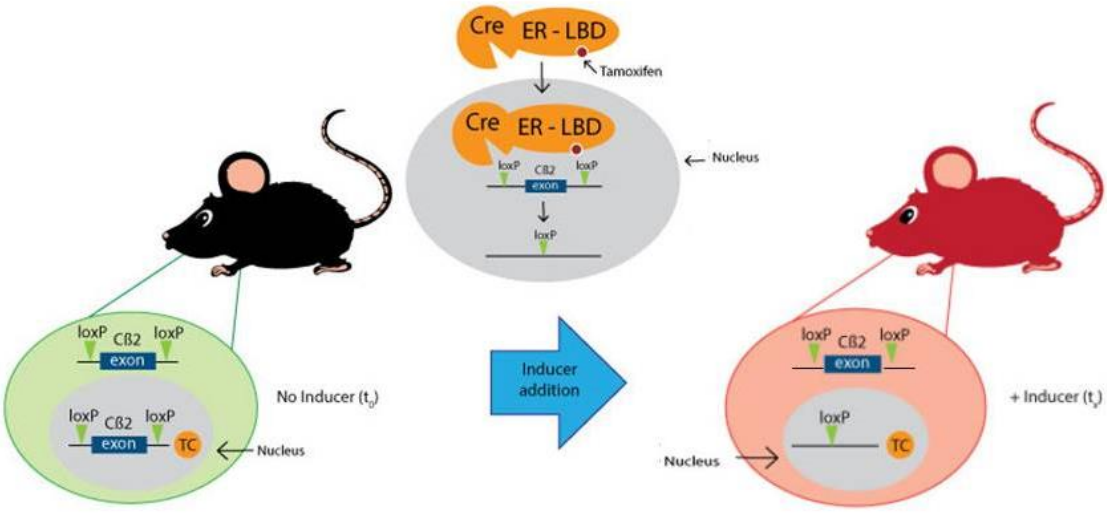

Figure 25. Inducible knockout model

Inducible gene inactivation is based on a mouse carrying a targeted exon (e.g. Cβ2) by loxP in cells expressing tamoxifen-dependent CreER recombinase (TC). CreER is fused with a mutated ligand binding domain (LDB) of the estrogain receptor (ER) and when tamoxifen (OHT) is absent CreER is present in the cytoplasm (mouse on the left). When the mouse is fed OHT (image in the middle), the binding to LBD results in the translocation of the recombinase into the nucleus, where it can recombine its loxP-flanked DNA substrate. This way mutagenesis can be achieved at any time in any specific tissue (mouse on the right).

The instrument is useful in gene studies and regarding human disease and is therefore a potential alternative to the approach used in this thesis. However, this technique can also allow for unwanted Cre activity and associated side effects, such as ectopic recombination based on transient Cre expression during development or potential toxic effects due to prolonged values of Cre activity (Loonstra et al., 2001; Schmidt, Taylor, Prigge, Barnett, & Capecchi, 2000). Nevertheless, the Inducible model has the ability to avoid results which may be typical for the constitutive KO approach, such as embryonic lethality, compensatory mechanisms or a complex phenotype (Coumoul & Deng, 2006; Deng, 2002; Friedberg & Meira, 2006; Weinstein, Yang, & Deng, 2000). However, the Inducible model is in a larger scale used as a strategy to enable the study of gene inactivation at various defined developmental stages, and as our mice appear healthy without the target gene present, the Induced KO approach may not be required to study Cβ2 function. Further, our mice line carries active Cre in all cells and tissues, creating KO in all cells when crossed with Flp delete mice. Having a mice line with Cre allows for a versatile use regarding future projects. For instance, there is the possibility of crossing Cre with delete mice linked to a promoter specific to T or B lymphocytes. This would allow us to study Cβ2 ablation in either T cells, B cells or other cells of interest (figure 26). In addition, if the mice with a promoter specific to T or B lymphocytes were crossed with CreER mice, and fed OHT, it would KO Cβ2 specifically in time (when fed OHT) and space (in particular cells such as T or B lymphocytes).

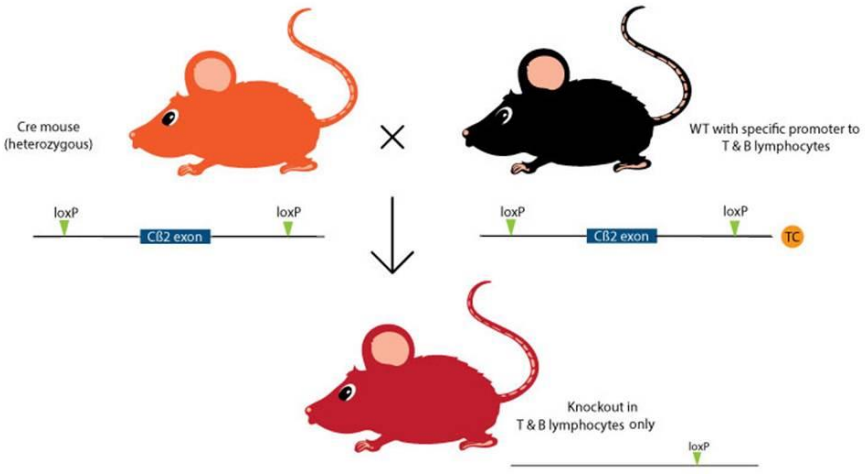

Figure 26. Possible model for knockout of T lymphocytes
A simplified scheme of a loxP hetrozygous mouse (upper mouse on the left) which is crossed with a mouse carrying a specific promoter for T and B lymhocytes (TC) (upper mouse on the right). Crossed together, these mice would get pups KO of Cβ2 specific for T and B lymphocytes.

5.2 Discussion of results

PKA is a main regulator of T and B cell growth and proliferation (Skalhegg et al., 2005). This together with the fact that Cβ2 is highly expressed in T, B and NK cells (A. Funderud et al., 2006; Orstavik et al., 2001) may suggest that Cβ2 holds a role in the regulation of immune cell activity and function and hence immune responses to various antigens. As a KO approach was used in order to study the role of Cβ2, we initially performed experiments to confirm ablation of Cβ2 DNA and protein. We showed that the Cβ2-specific DNA sequence was deleted in lymph node-, spleen- and thymus-cells. This was done by performing PCR with Cβ2 specific DNA primers. The primers were designed to detect Cβ2 wild type-, heterozygous or homozygous alleles and enabled us to decide which mice to use in the various experiments. To further assure that Cβ2 protein was ablated we performed immunoblotting using a pan anti-C subunit antibody. As Cβ2 runs with a relatively higher molecular mass, 47 kDa, in polyacrylamide (PAG) gels compared to other C subunits such as Cα1 and Cβ1 which runs at 40 kDa, it was possible to determine if the Cβ2 protein was expressed or not. This showed that the antiserum recognized both 40 kDa (Cα1/Cβ1) and 47 kDa (Cβ2) immunoreactive bands, while Cβ2 ablated cells only expressed the 40 kDa (Cα1/Cβ1) protein band. This demonstrated that Cβ2 protein in various immune cell tissues was deleted. In previous studies by Funderud et al., (2006, 2009) it was also found that the 47 kDa band was deleted in Cβall mice (ablation of all Cβ splice variants). This together with our results concluded that Cβ2 in lymphocytes is expressed as a 47 kDa protein.

Cβ2 protein ablation prompted us next to monitor catalytic activity, which was shown to be significantly reduced by 52, 39 and 37 %, in the Cβ2, ablated lymphocytes, splenocytes and thymocytes, respectively. This result was in line with Funderud et al. (2006; 2009) who showed that catalytic activity in Cβall KO was down-regulated by > 50 % (Ane Funderud et al., 2009; A. Funderud et al., 2006). When comparing Funderuds results with our findings we suggest that Cβ2 is the major PKA Cβ subunit in lymphocytes. Judging by quantity, it may further mean that the Cβ2 protein is involved in the regulation of immune cell growth and proliferation. Moreover, based on the role of cAMP and PKA in regulating T cell activation and proliferation, we speculated if Cβ2 ablation would be associated with spontaneous lymphocyte proliferation and hyper-activation upon stimulation through the antigen receptor complex. According to our results, this was not always the case. We initially stimulated a mixed population of cells with anti-CD3/CD28 coated beads. Whereas we did not monitor

any differences for lymph node cells, Cβ2 ablated splenocytes proliferated significantly more than wt cells in response to anti-CD3/CD28. As a mixed population of lymphocytes contains a variety of cells including NK cells, monocytes, macrophages and dendritic cells, these cells could together or alone influence our results on lymph node cells. Thus, to more precisely define the effect of Cβ2 ablation on lymph node cells we isolated and stimulated $CD4^+$ T cells from lymph nodes and spleen by CD3/CD28 coated beads. These experiments confirmed the results from the mixed cell population from lymph nodes and from spleen. We do not have any explanation for the discrepancy between the results obtained from mixed and $CD4^+$ splenocytes. Our results are also in line with the finding of Funderud et al., (2009) who did not observe any difference between splenocytes and lymph node cell proliferation upon anti-CD3/CD28 stimulation when isolated from Cβall KO. Moreover, Funderud could only identify hyper reactivity in Cα KO T cells, and not Cβall KO T cells suggesting that the two subunits may possess different roles in regulating immune cell responses. That Cβ may not be involved in the regulation of proliferation was further supported in that the activation marker CD69 was only increased in the Cα but not Cβ KO cells (Ane Funderud et al., 2009). Considering the results of Funderud and our results together, it may be suggested that Cβ2 does not play a vital role in regulating anti-CD3/CD28 induced proliferation in cells from neither lymph nodes nor spleen.

Why we observed that lymphocytes did not proliferate spontaneously nor show any hyper-reactivity to stimulation through the CD3/CD28 markers is not known. This was not expected based on the relative abundance of Cβ2 and the regulatory role of cAMP and PKA on lymphocyte activation. Considering the PKA holoenzyme as such in lymphocytes, previous research has demonstrated that the R to C subunit ratio is close to 1/1 in resting T lymphocytes (Skalhegg et al., 1994). When we monitored relative R subunit levels in Cβ2 ablated lymphocytes we found that immune reactive levels of RIα and RIIα were unaltered by Cβ2 ablation compared to wt lymphocytes. This may suggest that Cβ2 KO lymphocytes have an R to C ratio far above 1 as Cβ2 which makes up ^ 50 % of the C subunit in T cells (This thesis and Funderud et al 2009). This is indicative of a large overshoot of R subunit, which physiologically implies the Cβ2 KO lymphocytes contain PKA holoenzyme less sensitive to cAMP. As neither the protein levels for RIα nor RIIα were influenced by Cβ2 ablation this may further suggest that Cβ2 ablation renders both PKAI and PKAII insensitive to physiological levels of cAMP. To what extent this is the case and if it has a biological consequence remains to be verified. Finally, the fact that the R to C ratio is skewed upon Cβ2

KO may suggest that these lymphocytes are protected against the effect of cAMP and activation of PKA. Thus, if Cβ2 KO does not affect lymphocyte proliferation it may imply that Cβ2 possess activities that are not associated with regulating cell growth and division. This needs to be investigated further.

Incremental concentrations of glucose stimulates growth and proliferation independent of Cβ2 expression

Several studies have demonstrated that T cells deprived of glucose or T cells that do not possess normal glucose metabolism during activation are unable to proliferate normally (Bental & Deutsch, 1993; Fox et al., 2005; Macintyre et al., 2014; Oleszczak et al., 2012; Sena et al., 2013). PKA holds an important role in regulating glucose metabolism in liver and muscle cells (London et al., 2014; Schreyer et al., 2001). This combined with the results in this thesis prompted the idea that Cβ2 of PKA could hold a function in regulating glucose consumption.

Glucose concentrations (0 mM, 5 mM and 15 mM) and the rate of anti-CD3/CD28 induced proliferation were measured at 0 h, 24 h and 72 h after stimulation. We found that anti-CD3/CD28 stimulated Cβ2 KO and wt cells, grown in media absent of glucose, failed to increase their glucose uptake and had a proliferation rate close to non-stimulated cells. This was expected and in agreement with McIntyre et al., (2014) who published a similar result with T cells KO for GLUT 1 (Macintyre et al., 2014). It was also in line with McIver et al., (2008) who showed that T cells grown in media deprived of glucose would fail to proliferate unless the amino acid Glutamine was used as an alternate carbon source (MacIver et al., 2008).

As was demonstrated in the result, proliferation rate appeared low at 24 h for activated wt lymphocytes. The same observation was made for Cβ2 KO lymphocytes as well. A low proliferation rate was expected as it could indicate that cells were in the early stages of growth and proliferation (Carr et al., 2010; Frauwirth et al., 2002; Jacobs et al., 2008; R. Wang et al., 2011). The highest proliferation rate in wt lymphocytes was observed at 72 h. The same observation was made for Cβ2 KO lymphocytes. At this time point, glucose concentrations were 1 - 5 mM and we observed that the cells consumed the highest amount of glucose, even though it was not significant. Because this was observed in both wt and Cβ2 KO lymphocytes, it indicates that there were no differences between the groups regarding

proliferation rate and glucose consumption. We should have been able to see a spontaneous reaction in proliferation rate for lymphocytes KO for Cβ2 when compared to wt. This could have indicated that Cβ2 could have a function in regulation of glucose metabolism. However, this was not the case and unexpected given the role of PKA in regulation of glucose metabolism in liver and muscle cells. In light of our results, demonstrating that Cβ2 KO did not appear to influence lymphocyte proliferation it was not a surprise and may suggest that Cβ2 of PKA do not influence processes involving regulation such as energy formation through ATP formation by metabolism of glucose. Hence, it is tempting to speculate that Cβ2 is involved in other processes or that Cβ2 ablation is compensated by other C subunits. This is supported by Funderud et al., (2009) who showed that Cα most probably compensated for the ablation of Cβ as Cα and Cβ2 can form parts of the same PKAI holoenzyme (Funderud et al., 2009). However, to what extent this holds true needs further investigation.

Furthermore, we have confirmed a link between proliferation rate and glucose consumption in T cells. The highest proliferation rate for both wt and Cβ2 KO lymphocytes was at 72 h, when glucose concentration was 5 mM. This was not as a surprise as normal blood glucose levels in mammals are approximately 4 - 7 mM (Frayn, 2003; Saltiel & Kahn, 2001). This could indicate that activated T cells, even though in a stage of the clonal expansion phase and in need of glucose, prefer this level of glucose concentration for optimal function. This further highlights that a correct maintenance of glucose homeostasis is important for a functional immune system. According to MacIver et al., (2008), cells started proliferating at a very low concentration (0.1 mM) (MacIver et al., 2008). Our results demonstrate that a glucose concentration of 1 mM was sufficient to make both wt and Cβ2 KO lymphocytes proliferate and indicates that activated T cells have the ability to fully proliferate even at low glucose concentrations, like situations of hypoglycemia, and still being fully functional.

Furthermore, we showed that lymphocytes grown in 15 - 25 mM proliferated at the approximately same rate as cells grown in 1 - 5 mM glucose concentrations. According to Oleszcak et al., (2011), a blood glucose concentration of 200 mg/dL (11 mM) and 1000 mg/dL (55 mM) could cause apoptosis of lymphocytes (Oleszczak et al., 2012). And according to Otton et al., (2004) hyperglycemia in rats with 582 mg/dL (32.3 mM) showed apoptosis in lymphocytes (Otton, Soriano, Veriengia, & Curi, 2004). This could explain why our cells did not proliferate at a higher rate in higher concentrations of glucose, as it may be that they were on the edge of apoptosis. However, the level of proliferation could indicate that

the cells did not go through apoptosis, but that there are inhibiting factors that limit the proliferation rate when cells are grown in high glucose concentrations. Oleszcak et al., (2011) and others suggest that there could be mechanisms, which enables the cells to withstand harmful glucose concentrations, and that this could be linked to transport expression. They observed a drop in GLUT 1 and GLUT 3 expressions and an increase in GLUT 4 and suggest this to be a protective mechanism (Oleszczak et al., 2012; Stentz & Kitabchi, 2005). In our study we did not check for surface markers, but this would have been an interesting follow-up. Furthermore, Sena et al., (2012) found that glucose metabolism is only required for T cell activation so that pyruvate could fuel the mitochondria (Sena et al., 2013). This is in line with our results as we have shown that a glucose concentration of 1 – 5 mM appears as the optimal condition for proliferating T cells.

Pyruvate promotes cell proliferation in wt but not Cβ2 ablated T cells

When T cells are activated to proliferate, the glucose transporter Glut1 is upregulated and glucose is taken up. Glucose is converted to the 3-carbon pyruvate through the glycolysis (Maciolek et al., 2014). Sena et al (2013) and others also showed that pyruvate works as an extra nutrient source the cell can take advantage of (Maciolek et al., 2014; Sena et al., 2013). This prompted us to add pyruvate to the growth media and to investigate if this would influence T cell proliferation. Both wt and Cβ2 KO lymphocytes and splenocytes were stimulated with CD3/CD28 coated beads. Results showed that both lymphocytes and splenocytes from wt proliferated at a significantly higher rate than Cβ2 KO cells, in the presence of pyruvate. Our results were consistent with the observations by Sena et al., (2013) and others that pyruvate may act as a "quick" fuel (Sena et al. 2013: Maciolek et al., 2014). The fact that Cβ2 ablated lymphocytes and spenocytes proliferated at a significantly lower rate may indicate that Cβ2 possesses a regulatory link in the conversion and boosting effect of Pyruvate. The mechanism by which this occurs needs more investigation.

5.3 Conclusions

With our research as basis, this thesis demonstrates that:

- Cβ2 of PKA is ablated in lymph nodes, spleen and thymus from KO mice
- RIα and RIIα expressions are unaltered in Cβ2 KO cells from lymph nodes, spleen and thymus when compared to wt cells.
- There is a decreased cAMP-induced activity of PKA in Cβ2 KO lymphocytes, splenocytes and thymocytes.
- Cβ2 ablation influence CD3/CD28 stimulated proliferation rate in splenocytes but not lymphocytes
- Cβ2 ablation does not influence CD3/CD28 stimulated proliferation rate in splenocytes and lymphocytes, when cells are grown in incremental concentrations of glucose
- Cβ2 ablation does not influence CD3/CD28 stimulated proliferation rate in splenocytes and lymphocytes, when cells are grown inn media with pyruvate

Reference List

Bannard, O., Kraman, M., & Fearon, D. (2009). Pathways of memory CD8+ T-cell development. *European Journal of Immunology, 39*(8), 2083-2087. doi: 10.1002/eji.200939555

Bental, M., & Deutsch, C. (1993). Metabolic changes in activated T cells: an NMR study of human peripheral blood lymphocytes. *Magnetic Resonance in Medicine, 29*(3), 317-326.

Branda, C. S., & Dymecki, S. M. (2004). Talking about a revolution: The impact of site-specific recombinases on genetic analyses in mice. *Developmental Cell, 6*(1), 7-28.

Bremer, A. A., Devaraj, S., Afify, A., & Jialal, I. (2011). Adipose tissue dysregulation in patients with metabolic syndrome. *Journal of Clinical Endocrinology and Metabolism, 96*(11), E1782-1788. doi: 10.1210/jc.2011-1577

Bremer, A. A., & Jialal, I. (2013). Adipose tissue dysfunction in nascent metabolic syndrome. *Journal of Obesity, 2013*, 393192. doi: 10.1155/2013/393192

Brown, T. J., Ercolani, L., & Ginsberg, B. H. (1983). Properties and regulation of the T lymphocyte insulin receptor. *Journal of Receptor Research, 3*(4), 481-494.

Carr, E. L., Kelman, A., Wu, G. S., Gopaul, R., Senkevitch, E., Aghvanyan, A., . . . Frauwirth, K. A. (2010). Glutamine uptake and metabolism are coordinately regulated by ERK/MAPK during T lymphocyte activation. *Journal of Immunology, 185*(2), 1037-1044. doi: 10.4049/jimmunol.0903586

Cham, C. M., & Gajewski, T. F. (2005). Glucose availability regulates IFN-gamma production and p70S6 kinase activation in CD8+ effector T cells. *Journal of Immunology, 174*(8), 4670-4677.

Cochran, B. J., Bisoendial, R. J., Hou, L., Glaros, E., Rossy, J., Thomas, S. R., . . . Rye, K. A. (2014). Apolipoprotein A-I Increases Insulin Secretion and Production From Pancreatic beta-Cells via a G-Protein-cAMP-PKA-FoxO1-Dependent Mechanism. *Arteriosclerosis, Thrombosis, and Vascular Biology*. doi: 10.1161/atvbaha.114.304131

Coumoul, X., & Deng, C. X. (2006). RNAi in mice: a promising approach to decipher gene functions in vivo. *Biochimie, 88*(6), 637-643. doi: DOI 10.1016/j.biochi.2005.11.010

Deng, C. X. (2002). Tumor formation in Brca1 conditional mutant mice. *Environmental and Molecular Mutagenesis, 39*(2-3), 171-177.

DiSpirito, J. R., & Shen, H. (2010). Quick to remember, slow to forget: rapid recall responses of memory CD8+ T cells. *Cell Research, 20*(1), 13-23. doi: 10.1038/cr.2009.140

Emanuela, F., Grazia, M., Marco de, R., Maria Paola, L., Giorgio, F., & Marco, B. (2012). Inflammation as a Link between Obesity and Metabolic Syndrome. *J Nutr Metab, 2012*, 476380. doi: 10.1155/2012/476380

Ercolani, L., Lin, H. L., & Ginsberg, B. H. (1985). Insulin-induced desensitization at the receptor and postreceptor level in mitogen-activated human T-lymphocytes. *Diabetes, 34*(9), 931-937.

Esser, N., Legrand-Poels, S., Piette, J., Scheen, A. J., & Paquot, N. (2014). Inflammation as a link between obesity, metabolic syndrome and type 2 diabetes. *Diabetes Research and Clinical Practice, 105*(2), 141-150. doi: DOI 10.1016/j.diabres.2014.04.006

Feil, R. (2007). Conditional somatic mutagenesis in the mouse using site-specific recombinases. *Handbook of Experimental Pharmacology*(178), 3-28. doi: 10.1007/978-3-540-35109-2_1

Feil, R., Brocard, J., Mascrez, B., LeMeur, M., Metzger, D., & Chambon, P. (1996). Ligand-activated site-specific recombination in mice. *Proceedings of the National Academy of*

Sciences of the United States of America, 93(20), 10887-10890. doi: DOI 10.1073/pnas.93.20.10887
Feil, R., Wagner, J., Metzger, D., & Chambon, P. (1997). Regulation of Cre recombinase activity by mutated estrogen receptor ligand-binding domains. *Biochemical and Biophysical Research Communications, 237*(3), 752-757. doi: 10.1006/bbrc.1997.7124
Feil, S., Valtcheva, N., & Feil, R. (2009). Inducible Cre mice. *Methods in Molecular Biology, 530*, 343-363. doi: 10.1007/978-1-59745-471-1_18
Finlay, D., & Cantrell, D. A. (2011). Metabolism, migration and memory in cytotoxic T cells. *Nature Reviews: Immunology, 11*(2), 109-117. doi: 10.1038/nri2888
Foretz, M., Carling, D., Guichard, C., Ferre, P., & Foufelle, F. (1998). AMP-activated protein kinase inhibits the glucose-activated expression of fatty acid synthase gene in rat hepatocytes. *Journal of Biological Chemistry, 273*(24), 14767-14771. doi: DOI 10.1074/jbc.273.24.14767
Fox, C. J., Hammerman, P. S., & Thompson, C. B. (2005). Fuel feeds function: energy metabolism and the T-cell response. *Nature Reviews: Immunology, 5*(11), 844-852. doi: 10.1038/nri1710
Frauwirth, K. A., Riley, J. L., Harris, M. H., Parry, R. V., Rathmell, J. C., Plas, D. R., . . . Thompson, C. B. (2002). The CD28 signaling pathway regulates glucose metabolism. *Immunity, 16*(6), 769-777.
Frayn, K. N. (2003). *Metabolic Regulation A Human Perspective* (Second ed.): Blackwell Science Ltd.
Friedberg, E. C., & Meira, L. B. (2006). Database of mouse strains carrying targeted mutations in genes affecting biological responses to DNA damage Version 7. *DNA Repair (Amst), 5*(2), 189-209. doi: 10.1016/j.dnarep.2005.09.009
Funderud, A., Aas-Hanssen, K., Aksaas, A. K., Hafte, T. T., Corthay, A., Munthe, L. A., . . . Skålhegg, B. S. (2009). Isoform-specific regulation of immune cell reactivity by the catalytic subunit of protein kinase A (PKA). *Cellular Signalling, 21*(2), 274-281.
Funderud, A., Henanger, H. H., Hafte, T. T., Amieux, P. S., Orstavik, S., & Skalhegg, B. S. (2006). Identification, cloning and characterization of a novel 47 kDa murine PKA C subunit homologous to human and bovine Cbeta2. *BMC Biochemistry, 7*, 20. doi: 10.1186/1471-2091-7-20
Gerriets, V. A., & Rathmell, J. C. (2012). Metabolic pathways in T cell fate and function. *Trends in Immunology, 33*(4), 168-173. doi: 10.1016/j.it.2012.01.010
Guthrie, C. R., Skalhegg, B. S., & McKnight, G. S. (1997). Two novel brain-specific splice variants of the murine C beta gene of cAMP-dependent protein kinase. *Journal of Biological Chemistry, 272*(47), 29560-29565. doi: DOI 10.1074/jbc.272.47.29560
Härkönen, J. K. L. (2001). Cell Proliferation Assay by Using MicroBeta 3 H-Thymidine Incorporation. Retrieved 08.11.2014, 2014, from http://www.perkinelmer.com/CMSResources/Images/APP_Radiolabeled_Thymidine_Cell_Proliferation.pdf
Hånes, H., Graff-Iversen, S. & Meyer, H. . (2014, 11.04.2014). Overvekt og fedme hos voksne - faktaark med statistikk. 26.06.2012, from http://www.fhi.no/artikler/?id=44465
Indra, A. K., Warot, X., Brocard, J., Bornert, J. M., Xiao, J. H., Chambon, P., & Metzger, D. (1999). Temporally-controlled site-specific mutagenesis in the basal layer of the epidermis: comparison of the recombinase activity of the tamoxifen-inducible Cre-ER(T) and Cre-ER(T2) recombinases. *Nucleic Acids Research, 27*(22), 4324-4327.
Jacobs, S. R., Herman, C. E., MacIver, N. J., Wofford, J. A., Wieman, H. L., Hammen, J. J., & Rathmell, J. C. (2008). Glucose uptake is limiting in T cell activation and requires

CD28-mediated akt-dependent and independent pathways. *Journal of Immunology, 180*(7), 4476-4486.
Jiang, G. Q., & Zhang, B. B. (2003). Glucagon and regulation of glucose metabolism. *American Journal of Physiology-Endocrinology and Metabolism, 284*(4), E671-E678. doi: DOI 10.1152/ajpendo.00492.2002
Johnson, A. R., Milner, J. J., & Makowski, L. (2012). The inflammation highway: metabolism accelerates inflammatory traffic in obesity. *Immunological Reviews, 249*(1), 218-238. doi: 10.1111/j.1600-065X.2012.01151.x
Kammer, G. M. (2002). Deficient protein kinase a in systemic lupus erythematosus: a disorder of T lymphocyte signal transduction. *Annals of the New York Academy of Sciences, 968*, 96-105.
Kaneto, H., Xu, G., Song, K. H., Suzuma, K., Bonner-Weir, S., Sharma, A., & Weir, G. C. (2001). Activation of the hexosamine pathway leads to deterioration of pancreatic beta-cell function through the induction of oxidative stress. *Journal of Biological Chemistry, 276*(33), 31099-31104. doi: 10.1074/jbc.M104115200
Keith, B., Johnson, R. S., & Simon, M. C. (2012). HIF1α and HIF2α: sibling rivalry in hypoxic tumour growth and progression. *Nature Reviews: Cancer, 12*(1), 9-22.
Kvissel, A. K., Orstavik, S., Oistad, P., Rootwelt, T., Jahnsen, T., & Skalhegg, B. S. (2004). Induction of Cbeta splice variants and formation of novel forms of protein kinase A type II holoenzymes during retinoic acid-induced differentiation of human NT2 cells. *Cellular Signalling, 16*(5), 577-587.
Lea, T. (2008). *Immunologi og immunologiske teknikker* (Vol. 2. Opplag): Fagbokforlaget Vigmostad & Bjørke AS.
Levitzki, A. (1988). From Epinephrine to Cyclic-Amp. *Science, 241*(4867), 800-806. doi: DOI 10.1126/science.2841758
Levy, F. O., Rasmussen, A. M., Tasken, K., Skalhegg, B. S., Huitfeldt, H. S., Funderud, S., . . . Hansson, V. (1996). Cyclic AMP-dependent protein kinase (cAK) in human B cells: Co-localization of type I cAK (RI alpha C-2(2)) with the antigen receptor during antiimmunoglobulin-induced B cell activation. *European Journal of Immunology, 26*(6), 1290-1296. doi: DOI 10.1002/eji.1830260617
LifeTechnologies. (2014a). Dynabeads Mouse T-Avtivator CD3/CD28 for T-Cell Expansion and Activation. Retrieved 08.11.2014, 2014, from http://www.lifetechnologies.com/order/catalog/product/11452D?ICID=search-11452d
LifeTechnologies. (2014b). Dynabeads® Mouse T-Activator CD3/CD28. Retrieved 08.11.2014, 2014, from http://tools.lifetechnologies.com/content/sfs/manuals/dynamouse_tactivatorCD3_CD28_man.pdf
LifeTechnologies. (2014c, 03.2012). Negative Cell Isolation of Truly Untouched Cells. Retrieved 08.11.2014, 2014, from http://www.lifetechnologies.com/no/en/home/life-science/cell-analysis/cell-isolation-and-expansion/cell-isolation/negative-cell-isolation.html
London, E., Nesterova, M., Sinaii, N., Szarek, E., Chanturiya, T., Mastroyannis, S. A., . . . Stratakis, C. A. (2014). Differentially regulated protein kinase A (PKA) activity in adipose tissue and liver is associated with resistance to diet-induced obesity and glucose intolerance in mice that lack PKA regulatory subunit type IIalpha. *Endocrinology, 155*(9), 3397-3408. doi: 10.1210/en.2014-1122
Loonstra, A., Vooijs, M., Beverloo, H. B., Allak, B. A., van Drunen, E., Kanaar, R., . . . Jonkers, J. (2001). Growth inhibition and DNA damage induced by Cre recombinase in mammalian cells. *Proceedings of the National Academy of Sciences of the United States of America, 98*(16), 9209-9214. doi: 10.1073/pnas.161269798

Luo, G., Kong, X., Lu, L., Xu, X., Wang, H., & Ma, X. (2013). Glucagon-like peptide 1 potentiates glucotoxicity-diminished insulin secretion via stimulation of cAMP-PKA signaling in INS-1E cells and mouse islets. *International Journal of Biochemistry and Cell Biology, 45*(2), 483-490. doi: 10.1016/j.biocel.2012.11.016

Macintyre, A. N., Gerriets, V. A., Nichols, A. G., Michalek, R. D., Rudolph, M. C., Deoliveira, D., . . . Rathmell, J. C. (2014). The glucose transporter Glut1 is selectively essential for CD4 T cell activation and effector function. *Cell Metab, 20*(1), 61-72. doi: 10.1016/j.cmet.2014.05.004

Maciolek, J. A., Pasternak, J. A., & Wilson, H. L. (2014). Metabolism of activated T lymphocytes. *Current Opinion in Immunology, 27*, 60-74. doi: 10.1016/j.coi.2014.01.006

MacIver, N. J., Jacobs, S. R., Wieman, H. L., Wofford, J. A., Coloff, J. L., & Rathmell, J. C. (2008). Glucose metabolism in lymphocytes is a regulated process with significant effects on immune cell function and survival. *Journal of Leukocyte Biology, 84*(4), 949-957. doi: Doi 10.1189/Jlb.0108024

McLaughlin, T., Liu, L. F., Lamendola, C., Shen, L., Morton, J., Rivas, H., . . . Engleman, E. (2014). T-Cell Profile in Adipose Tissue Is Associated With Insulin Resistance and Systemic Inflammation in Humans. *Arteriosclerosis, Thrombosis, and Vascular Biology*. doi: 10.1161/atvbaha.114.304636

Mestas, J., & Hughes, C. C. (2004). Of mice and not men: differences between mouse and human immunology. *Journal of Immunology, 172*(5), 2731-2738.

Metzger, D., Clifford, J., Chiba, H., & Chambon, P. (1995). Conditional site-specific recombination in mammalian cells using a ligand-dependent chimeric Cre recombinase. *Proceedings of the National Academy of Sciences of the United States of America, 92*(15), 6991-6995.

Michalek, R. D., Gerriets, V. A., Nichols, A. G., Inoue, M., Kazmin, D., Chang, C. Y., . . . Rathmell, J. C. (2011). Estrogen-related receptor-alpha is a metabolic regulator of effector T-cell activation and differentiation. *Proceedings of the National Academy of Sciences of the United States of America, 108*(45), 18348-18353. doi: 10.1073/pnas.1108856108

Muth, N. D. (2009). What are the guidelines for percentage of body fat loss? Retrieved 08.11.2014, from http://www.acefitness.org/acefit/healthy-living-article/60/112/what-are-the-guidelines-for-percentage-of/

nhi.no. (2013a, 17.10.2013). Hva er hiv? Retrieved 08.11.2014, 2014, from http://nhi.no/pasienthandboka/infeksjoner/hiv-og-aids/hiv-hva-er-det-11544.html

nhi.no. (2013b, 19.08.2013). Systemisk lupus erytematosus (SLE). Retrieved 08.11.2014, 2014, from http://nhi.no/pasienthandboka/muskel-skjelett/ulike-muskelsykdommer/systemisk-lupus-erytematosus-3186.html?page=all

O'Neill, L. A., & Hardie, D. G. (2013). Metabolism of inflammation limited by AMPK and pseudo-starvation. *Nature, 493*(7432), 346-355. doi: 10.1038/nature11862

Oksvold, M. P., Funderud, A., Kvissel, A. K., Skarpen, E., Henanger, H., Huitfeldt, H. S., . . . Orstavik, S. (2008). Epidermal growth factor receptor levels are reduced in mice with targeted disruption of the protein kinase A catalytic subunit. *BMC Cell Biology, 9*, 16. doi: 10.1186/1471-2121-9-16

Oleszczak, B., Szablewski, L., & Pliszka, M. (2012). The effect of hyperglycemia and hypoglycemia on glucose transport and expression of glucose transporters in human lymphocytes B and T: an in vitro study. *Diabetes Research and Clinical Practice, 96*(2), 170-178. doi: 10.1016/j.diabres.2011.12.012

Orstavik, S., Funderud, A., Hafte, T. T., Eikvar, S., Jahnsen, T., & Skalhegg, B. S. (2005). Identification and characterization of novel PKA holoenzymes in human T lymphocytes. *Febs j, 272*(7), 1559-1567. doi: 10.1111/j.1742-4658.2005.04568.x

Orstavik, S., Reinton, N., Frengen, E., Langeland, B. T., Jahnsen, T., & Skalhegg, B. S. (2001). Identification of novel splice variants of the human catalytic subunit Cbeta of cAMP-dependent protein kinase. *European Journal of Biochemistry, 268*(19), 5066-5073.

Otton, R., Soriano, F. G., Veriengia, R., & Curi, R. (2004). Diabetes induces apoptosis in lymphocytes. *Journal of Endocrinology, 182*(1), 145-156. doi: DOI 10.1677/joe.0.1820145

Ouedraogo, R., Wu, X., Xu, S. Q., Fuchsel, L., Motoshima, H., Mahadev, K., . . . Goldstein, B. J. (2006). Adiponectin suppression of high-glucose-induced reactive oxygen species in vascular endothelial cells: evidence for involvement of a cAMP signaling pathway. *Diabetes, 55*(6), 1840-1846. doi: 10.2337/db05-1174

Palmeira, C. M., Rolo, A. P., Berthiaume, J., Bjork, J. A., & Wallace, K. B. (2007). Hyperglycemia decreases mitochondrial function: the regulatory role of mitochondrial biogenesis. *Toxicology and Applied Pharmacology, 225*(2), 214-220. doi: 10.1016/j.taap.2007.07.015

Palomer, X., Salvado, L., Barroso, E., & Vazquez-Carrera, M. (2013). An overview of the crosstalk between inflammatory processes and metabolic dysregulation during diabetic cardiomyopathy. *International Journal of Cardiology, 168*(4), 3160-3172. doi: 10.1016/j.ijcard.2013.07.150

Papathanassoglou, E., El-Haschimi, K., Li, X. C., Matarese, G., Strom, T., & Mantzoros, C. (2006). Leptin receptor expression and signaling in lymphocytes: kinetics during lymphocyte activation, role in lymphocyte survival, and response to high fat diet in mice. *Journal of Immunology, 176*(12), 7745-7752.

Pearce, E. L., Walsh, M. C., Cejas, P. J., Harms, G. M., Shen, H., Wang, L. S., . . . Choi, Y. (2009). Enhancing CD8 T-cell memory by modulating fatty acid metabolism. *Nature, 460*(7251), 103-107. doi: 10.1038/nature08097

Powers, G. (2005). *Human Nutrition* (H. J. P. Cathrine A. Geissler Ed. Eleventh Edition ed.).

Procaccini, C., Jirillo, E., & Matarese, G. (2012). Leptin as an immunomodulator. *Molecular Aspects of Medicine, 33*(1), 35-45. doi: 10.1016/j.mam.2011.10.012

Runge&Patterson. (2006). *Principles of Molecular Medicine*. Humana Press.

Sakaguchi, S., Miyara, M., Costantino, C. M., & Hafler, D. A. (2010). FOXP3+ regulatory T cells in the human immune system. *Nature Reviews: Immunology, 10*(7), 490-500. doi: 10.1038/nri2785

Saltiel, A. R., & Kahn, C. R. (2001). Insulin signalling and the regulation of glucose and lipid metabolism. *Nature, 414*(6865), 799-806.

Saucillo, D. C., Gerriets, V. A., Sheng, J., Rathmell, J. C., & Maciver, N. J. (2014). Leptin metabolically licenses T cells for activation to link nutrition and immunity. *Journal of Immunology, 192*(1), 136-144. doi: 10.4049/jimmunol.1301158

Schillace, R. V., Andrews, S. F., Galligan, S. G., Burton, K. A., Starks, H. J., Bouwer, H. G., . . . Carr, D. W. (2005). The role of protein kinase A anchoring via the RII alpha regulatory subunit in the murine immune system. *Journal of Immunology, 174*(11), 6847-6853.

Schmidt, E. E., Taylor, D. S., Prigge, J. R., Barnett, S., & Capecchi, M. R. (2000). Illegitimate Cre-dependent chromosome rearrangements in transgenic mouse spermatids. *Proceedings of the National Academy of Sciences of the United States of America, 97*(25), 13702-13707. doi: 10.1073/pnas.240471297

Schreyer, S. A., Cummings, D. E., McKnight, G. S., & LeBoeuf, R. C. (2001). Mutation of the RIIbeta subunit of protein kinase A prevents diet-induced insulin resistance and dyslipidemia in mice. *Diabetes, 50*(11), 2555-2562.

Schwencke, C., Yamamoto, M., Okumura, S., Toya, Y., Kim, S. J., & Ishikawa, Y. (1999). Compartmentation of cyclic adenosine 3',5'-monophosphate signaling in caveolae. *Molecular Endocrinology, 13*(7), 1061-1070. doi: 10.1210/mend.13.7.0304

Semenza, G. L. (2012). Hypoxia-inducible factors in physiology and medicine. *Cell, 148*(3), 399-408. doi: 10.1016/j.cell.2012.01.021

Sena, L. A., Li, S., Jairaman, A., Prakriya, M., Ezponda, T., Hildeman, D. A., . . . Chandel, N. S. (2013). Mitochondria are required for antigen-specific T cell activation through reactive oxygen species signaling. *Immunity, 38*(2), 225-236. doi: 10.1016/j.immuni.2012.10.020

Shi, L. Z., Wang, R., Huang, G., Vogel, P., Neale, G., Green, D. R., & Chi, H. (2011). HIF1alpha-dependent glycolytic pathway orchestrates a metabolic checkpoint for the differentiation of TH17 and Treg cells. *Journal of Experimental Medicine, 208*(7), 1367-1376. doi: 10.1084/jem.20110278

Skalhegg, B. S., Funderud, A., Henanger, H. H., Hafte, T. T., Larsen, A. C., Kvissel, A. K., . . . Orstavik, S. (2005). Protein kinase A (PKA)--a potential target for therapeutic intervention of dysfunctional immune cells. *Current Drug Targets, 6*(6), 655-664.

Skalhegg, B. S., Landmark, B., Foss, K. B., Lohmann, S. M., Hansson, V., Lea, T., & Jahnsen, T. (1992). Identification, purification, and characterization of subunits of cAMP-dependent protein kinase in human testis. Reverse mobilities of human RII alpha and RII beta on sodium dodecyl sulfate-polyacrylamide gel electrophoresis compared with rat and bovine RIIs. *Journal of Biological Chemistry, 267*(8), 5374-5379.

Skalhegg, B. S., Rasmussen, A. M., Tasken, K., Hansson, V., Jahnsen, T., & Lea, T. (1994). Cyclic AMP sensitive signalling by the CD28 marker requires concomitant stimulation by the T-cell antigen receptor (TCR/CD3) complex. *Scandinavian Journal of Immunology, 40*(2), 201-208.

Skalhegg, B. S., & Tasken, K. (2000). Specificity in the cAMP/PKA signaling pathway. Differential expression,regulation, and subcellular localization of subunits of PKA. *Frontiers in Bioscience, 5*, D678-693.

St-Onge, L., Furth, P. A., & Gruss, P. (1996). Temporal control of the Cre recombinase in transgenic mice by a tetracycline responsive promoter. *Nucleic Acids Research, 24*(19), 3875-3877.

Stentz, F. B., & Kitabchi, A. E. (2003). Activated T lymphocytes in Type 2 diabetes: implications from in vitro studies. *Current Drug Targets, 4*(6), 493-503.

Stentz, F. B., & Kitabchi, A. E. (2005). Hyperglycemia-induced activation of human T-lymphocytes with de novo emergence of insulin receptors and generation of reactive oxygen species. *Biochemical and Biophysical Research Communications, 335*(2), 491-495. doi: 10.1016/j.bbrc.2005.07.109

Tasken, K., & Aandahl, E. M. (2004). Localized effects of cAMP mediated by distinct routes of protein kinase A. *Physiological Reviews, 84*(1), 137-167. doi: 10.1152/physrev.00021.2003

Torgersen, K. M., Vaage, J. T., Levy, F. O., Hansson, V., Rolstad, B., & Tasken, K. (1997). Selective activation of cAMP-dependent protein kinase type I inhibits rat natural killer cell cytotoxicity. *Journal of Biological Chemistry, 272*(9), 5495-5500.

Torgersen, K. M., Vang, T., Abrahamsen, H., Yaqub, S., & Tasken, K. (2002). Molecular mechanisms for protein kinase A-mediated modulation of immune function. *Cellular Signalling, 14*(1), 1-9.

Uhler, M. D., Carmichael, D. F., Lee, D. C., Chrivia, J. C., Krebs, E. G., & Mcknight, G. S. (1986). Isolation of Cdna Clones Coding for the Catalytic Subunit of Mouse Camp-Dependent Protein-Kinase. *Proceedings of the National Academy of Sciences of the United States of America, 83*(5), 1300-1304. doi: DOI 10.1073/pnas.83.5.1300

Uhler, M. D., Chrivia, J. C., & McKnight, G. S. (1986). Evidence for a second isoform of the catalytic subunit of cAMP-dependent protein kinase. *Journal of Biological Chemistry, 261*(33), 15360-15363.

Vander Heiden, M. G., Cantley, L. C., & Thompson, C. B. (2009). Understanding the Warburg effect: the metabolic requirements of cell proliferation. *Science, 324*(5930), 1029-1033. doi: 10.1126/science.1160809

Viardot, A., Heilbronn, L. K., Samocha-Bonet, D., Mackay, F., Campbell, L. V., & Samaras, K. (2012). Obesity is associated with activated and insulin resistant immune cells. *Diabetes/Metabolism Research and Reviews, 28*(5), 447-454. doi: 10.1002/dmrr.2302

Wang, F., Zhao, Y., Niu, Y., Wang, C., Wang, M., Li, Y., & Sun, C. (2012). Activated glucose-6-phosphate dehydrogenase is associated with insulin resistance by upregulating pentose and pentosidine in diet-induced obesity of rats. *Hormone and Metabolic Research, 44*(13), 938-942. doi: 10.1055/s-0032-1323727

Wang, R., Dillon, C. P., Shi, L. Z., Milasta, S., Carter, R., Finkelstein, D., . . . Green, D. R. (2011). The transcription factor Myc controls metabolic reprogramming upon T lymphocyte activation. *Immunity, 35*(6), 871-882. doi: 10.1016/j.immuni.2011.09.021

Wang, R., & Green, D. R. (2012). Metabolic reprogramming and metabolic dependency in T cells. *Immunological Reviews, 249*(1), 14-26. doi: 10.1111/j.1600-065X.2012.01155.x

Warburg, O., Wind, F., & Negelein, E. (1927). The Metabolism of Tumors in the Body. *Journal of General Physiology, 8*(6), 519-530.

Weinstein, M., Yang, X., & Deng, C.-X. (2000). Functions of mammalian Smad genes as revealed by targeted gene disruption in mice. *Cytokine and Growth Factor Reviews, 11*(1–2), 49-58. doi: http://dx.doi.org/10.1016/S1359-6101(99)00028-3

WHO. (2014a, 08.11.2014). BMI classification. from http://apps.who.int/bmi/index.jsp?introPage=intro_3.html

WHO. (2014b). Chronic diseases and health promotion Part Two. The urgent need for action Risk factor projections: overweight and obesity. from http://www.who.int/chp/chronic_disease_report/part2_ch1/en/index16.html

WHO. (2014c, 08.2014). Obesity and overweight. Retrieved 08.11.2014, from http://www.who.int/mediacentre/factsheets/fs311/en/

WHO. (2014d). Part Two. The urgent need for action Chapter One. Chronic diseases: causes and health impact Projections of future deaths. Retrieved 08.11.2014, from http://www.who.int/chp/chronic_disease_report/part2_ch1/en/index18.html

Wiemann, S., Kinzel, V., & Pyerin, W. (1991). Isoform C beta 2, an unusual form of the bovine catalytic subunit of cAMP-dependent protein kinase. *Journal of Biological Chemistry, 266*(8), 5140-5146.

Yu, Y., Liu, Y., Shi, F. D., Zou, H., Matarese, G., & La Cava, A. (2013). Cutting edge: Leptin-induced RORgammat expression in CD4+ T cells promotes Th17 responses in systemic lupus erythematosus. *Journal of Immunology, 190*(7), 3054-3058. doi: 10.4049/jimmunol.1203275

Yudkin, J. S., Stehouwer, C. D., Emeis, J. J., & Coppack, S. W. (1999). C-reactive protein in healthy subjects: associations with obesity, insulin resistance, and endothelial dysfunction: a potential role for cytokines originating from adipose tissue? *Arteriosclerosis, Thrombosis, and Vascular Biology, 19*(4), 972-978.

Zhang, Y., Riesterer, C., Ayrall, A. M., Sablitzky, F., Littlewood, T. D., & Reth, M. (1996). Inducible site-directed recombination in mouse embryonic stem cells. *Nucleic Acids Research*, *24*(4), 543-548.

Zimmet, P., Alberti, K. G. M. M., & Shaw, J. (2001). Global and societal implications of the diabetes epidemic. *Nature*, *414*(6865), 782-787.

Appendix A - List of Reagents and Materials

Name	Supplier	Catalog #
1 Kb DNA ladder stock	Life Technologies	15615-024
[^{3}H]-Thymidine (5 mCi/mL)	Nærliens	NET027X005MC
Antibody: Mouse c-mono: 1:100	BD Transduction Laboratories	610980/81
Antibody: RIα Mouse monoclonal 1:100	BD Transduction Laboratories	610166
Antibody: RIIα Mouse monoclonal 1:100	BD Transduction Laboratories	612243
Antibody: GADPH rabbit polyclonal 1:1000	Sigma	G9545
Criterion Precast Gels SDS-PAGE 12.5 %	Bio-Rad	345-0014
cyclic Adenosine Monophosphate (cAMP)	Sigma	A9501
Deoxyribonucleotide Triphosphate (dNTPmix)	Finnzymes	F-560XL
Dulbecco`s Phosphate Buffered Saline	Sigma	D8537
DyNAzyme	Thermo Scientific	F-501L
Dynabeads Mouse T-Activator CD3/CD28	Life Technologies	11452D
Dynabeads Untouched™ Mouse C cells	Life Technologies	11415D
D-(+)-Glucose Solution 45 % 2. 5 stock	Sigma	G8769
Ethidium Bromide	Sigma	E8751
Ethylenediaminetetraacetic acid (EDTA)	BDH Biochemical	443885J
Expand High Fidelity PCR System	Roche	03300226001
Fetal Bovine Serum (FBS)	Sigma	F7524
Ficoll	VWR	437092S
HRP conjugate anti-mouse secondary antibody	BP Biomedicals	
Kemptide peptide	Sigma	60645
L-Glutamine 200mM	Sigma	G7513
MagNa Pure LC DNA Isolation Kit	Roche	05197686001
MagNa Pure LC DNA Isolation Kit II Tissue	Roche	03186229001
Methanol	Emsure	603-001-00-X
Microscint ™ O	PerkinElmer	6013611
Molecular Biology Grade Agarose DNA Pure Grade 500g	VWR	443666A
Non essential amino acids	Gibco BRL	11140-035
Optifluor	PerkinElmer	6013199

Orange G	Sigma	16230
Penicillin Streptomycin Solution Stabilized	Sigma	P4458
Phenylmethanesulfonylfluoride	Sigma	P7626
Phosphate Buffered Saline	Sigma	P4417
Phosphate Buffered Saline	Sigma	SLBG4621V
Phosphocellulose paper	P81 Whatman	3698915
Phosphoric Acid	Sigma	79622
Pierce BCA Protein Assay Prod A	Thermo Scientific	23223
Pierce BCA Protein Assay Prod B	Thermo Scientific	23224
Pierce Enhanced chemiluminescence (ECL) kit	Thermo Scientific	34080
PKA-specific inhibitor (PKI)	Sigma	P-6062
PKA-specific phosphotransferase [γ-32P] ATP	PerkinElmer	NEG508X250UC
Precision Plus Protein Standards, Dual Color Standard	Bio-Rad	161-0374
Primer (forward): 5' tgtaggtcctgctgtatgcttgtctaccc Primer (reverse): 5' cttgctccttagccatttcttactccagc Primer (reverse): 5' tatttgcctgtctacatcatgcgtgtcag		
Polyvinylidene Fluoride Membrane (PVDF)	Immobilion-P	IPV00010
Proteinase Inhibitor	Sigma	P8340
Red Blood Cell Lysing buffer	Sigma	R7757
RPMI 1640	Gibco	11879-020
RPMI 1640	Sigma	R0883
Scintillation liquid	PerkinElmer	6013611
Secondary antibodies anti-mouse to C-mono	Cappel	55563
Sodium Duodecyl Sulfate	Bio-Rad	161-0302
Sodium Fluoride	VWR International	56420-250
Sodium Pyrophosphate	VWR International	16591-25
Sodium pyruvate 100 mM	Gibco BRL	11360-039
Sodium Vanadate	Sigma	6508
SuperSignal West Dura Extended Duration Substrate kit	Thermo Scientific	34076
SuperSignal West Pico Chemiluminescent	Thermo Scientific	34080
SuperSignal West Dura Extended Duration Substrate kit	Thermo Sientific	34076
SybrSafe	Life Technologies	s33102
Tris (hydroxymethyl) aminomethane pH 7.4	VWR International	TD12024319

Triton	Sigma	69H0147
Trypan Blue Stain 0.4 %	Life Technologies	T10282
Whatman paper sheets	Sigma	1003-917

Materials

96 well plate	Costar	3799
96 well filter plate	Perkin Elmer	6005174
Cell strainer (70 µm)	Falcon	352350
Cell harvester	PerkinElmer	C961241
Countess® automated cell counter	Life Technologies	C10227
Countess®Cell counting chamber slides	Life Technologies	C10228
Filter (0, 2 µm)	Life Sciences	PN 4612
Glucose test apparatus ACCU-CHEK Aviva	Roche	03532321004
Round bottomed plate	Costar	3799
Scintillation counter	Packard	1282
Slide-A-Lyzer Cassette	Thermo Scientific	66130
Syringe	BD Plastipak	300185
Syringe	Sterican	4657527
Syringe Filter	Life Sciences	7936179E
Test strips	Roche	06453970

Development of a PKACβ2 conditional Knock-out

Mouse screening report

genOway/PP/SKA1-PKACβ2/040506

30 November 2007

www.genoway.com

genOway - Head Office: 181 avenue Jean Jaurès • 69362 Lyon cedex 07 • France • Phone: +33 (0)4 37 65 41 00 • Fax: +33 (0)4 37 65 41 01
genOway Germany GmbH : Grundstrasse 16 • 20257 Hamburg • Germany • Phone: +49 (0)40 40 19 71 00 • Fax: +49 (0)40 43 20 82 61
e-mail: info@genoway.com • website: www.genoway.com

Table of contents

Author: This document was written by Dr. Hélène TONOLI-CATEZ, *Project Leader* at genOway

genOway - Head Office
181 avenue Jean Jaurès
69362 Lyon cedex 07
France
Tel : +33 (0)4 37 65 41 00
Fax : +33 (0)4 37 65 41 01
e-mail : info@genoway.com

1 GENOTYPING OF THE *PKACβ2* CONDITIONAL AND CONSTUTUTIVE KNOCK-OUT MOUSE LINES

The Flp-mediated excision enables the deletion of the neomycin cassette, resulting in a *PKACβ2* conditional Knock-out allele or *PKACβ2* floxed allele. This deletion has been performed *in vivo*, by breeding the recombined animals with ubiquitous Flp-recombinase expressing deleter mice (see Final report sent on 30 November 2007).

The Cre-mediated excision enables the deletion of the exon 1β2, resulting in a *PKACβ2* constitutive Knock-out allele. This deletion can been performed *in vivo*, by breeding the recombined animals with Cre-recombinase expressing deleter mice.

PCR and Southern blot screening have been established to enable the wild type, the Neo-deleted allele (*PKACβ2* floxed allele) and the Knock-out allele to be clearly distinguished.

1-1 PCR SCREENING STRATEGY FOR THE GENOTYPING OF THE PKACβ2 CONDITIONAL KNOCK-OUT LINE

This PCR is performed using a forward primer GX4475 hybridizing upstream the FRT flanked neomycin cassette and a reverse primer GX4476 hybridizing downstream of the FRT flanked neomycin selection cassette (see figure 1). Because of its localisation, this primer pair allows allows the distinction of the Flp-mediated neomycin-deleted floxed allele from the wild-type allele.

The conditional Knock-out allele (or floxed allele) should yield an amplification product of 767 pb using the above primer pair whereas the wild-type allele should yield an amplification product of 660 pb.

The sequence of the primers and the optimised PCR conditions are listed in tables 1 and 2.

Primer name	Primer sequence 5'-3'	Expected size of PCR product in	
		Wild-type allele	Flp-excised allele
GX4475-SKA1-R	GAGAGCCAGTCAAGGGAACTGAATGC	660 bp	767 bp
GX4476-SKA1-S	TGTTGCTTGGCTAATGACTGTCAAAGC		

Table 1: Primers for the PCR screening for the detection of the *PKACβ2* floxed allele

Reaction mix			Reaction conditions			
Genomic DNA	10	ng	**Step**	**Temp.**	**Time**	**Cycles**
Primers	each 15	pmol	Denaturing	94°C	120s	1 x
dNTPs	0.5	mM	Denaturing	94°C	30s	35 x
Reaction buffer 3	0.1	Vol	Annealing	65°C	30s	
Taq Long expand (Roche)	2.6	U	Extension	68°C	300s	
Reaction Volume	50.0	µl	Completion	68°C	480s	1 x

Table 2: Optimised PCR conditions for the detection of the *PKACβ2* floxed allele

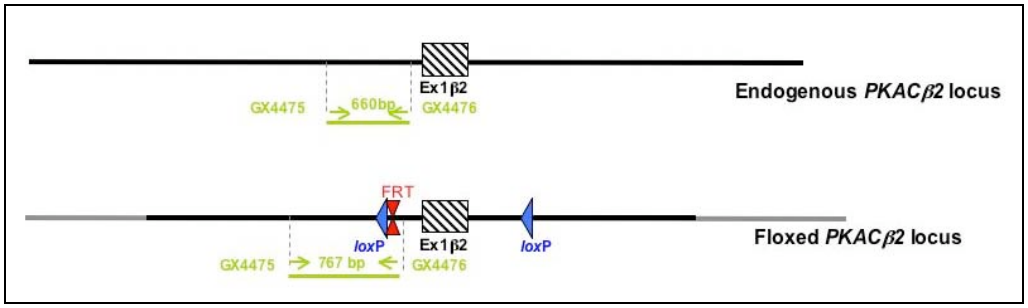

Figure 1: PCR genotyping of the *PKACβ2* floxed mouse line. *Schematic representation of the PKACβ2 alleles with the binding sites of the screening primers is shown.*

1-2 PCR SCREENING STRATEGY FOR THE GENOTYPING OF THE PKACβ2 CONSTITUTIVE KNOCK-OUT LINE

This PCR is performed using a forward primer GX4473 hybridizing upstream of the targeting vector homology sequence and a reverse primer GX4474 hybridizing downstream of the *loxP* site (see figure 2). Because of its localization, this primer pair allows to distinguish the *PKACβ2* Cre-deleted Knock-out allele from the *PKACβ2* wild-type allele.

The Knock-out allele should yield an amplification product of 2.6 kb using the above primer pair whereas the wild-type allele should yield an amplification product of 5.3 kb.

The sequence of the primers and the optimised PCR conditions are listed in tables 3 and 4.

Primer name	Primer sequence 5'-3'	Expected size of PCR product in	
		Wild-type allele	Knock-out allele
GX4473	AAGGTCCGACCATCTGAAGGAAAGC	5346 bp	2551 bp
GX4474	TGCTCCTTAGCCATTTCTTACTCCAGC		

Table 3: Primers for the PCR screening for the detection of the *PKACβ2* Knock-out allele

Reaction mix			Reaction conditions			
Genomic DNA	10	ng	**Step**	**Temp.**	**Time**	**Cycles**
Primers	each 15	pmol	Denaturing	94°C	120s	1 x
dNTPs	0.5	mM	Denaturing	94°C	30s	35 x
Reaction buffer 3	0.1	Vol	Annealing	65°C	30s	
Expand HF Polymerase (Roche)	2.6	U	Extension	68°C	420s	
Reaction Volume	50.0	µl	Completion	72°C	480s	1 x

Table 4: Optimised PCR conditions for the detection of the *PKACβ2* Knock-out allele

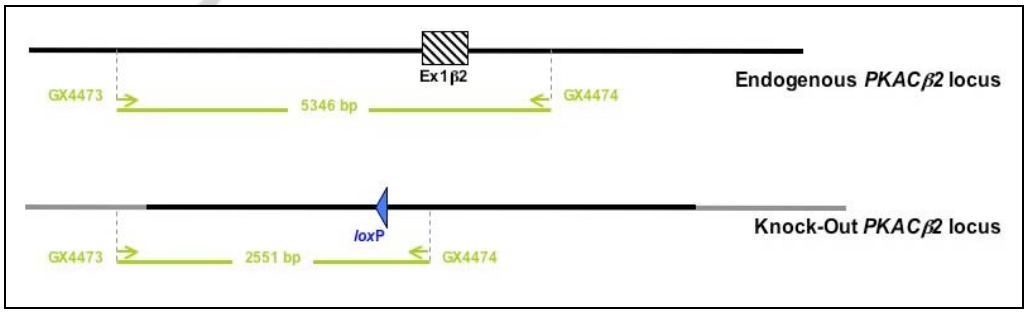

Figure 2: PCR genotyping of the *PKACβ2* Knock-out mouse line. *(A) Schematic representation of the PKACβ2 alleles with the binding sites of the screening primers shown.*

1-3 DETECTION OF HOMOZYGOUS KNOCK-OUT ANIMALS BY PCR

To screen for the homozygous animals, the F2 progeny will be screened using a PCR specific to wild-type *PKACβ2* allele (figure 3).

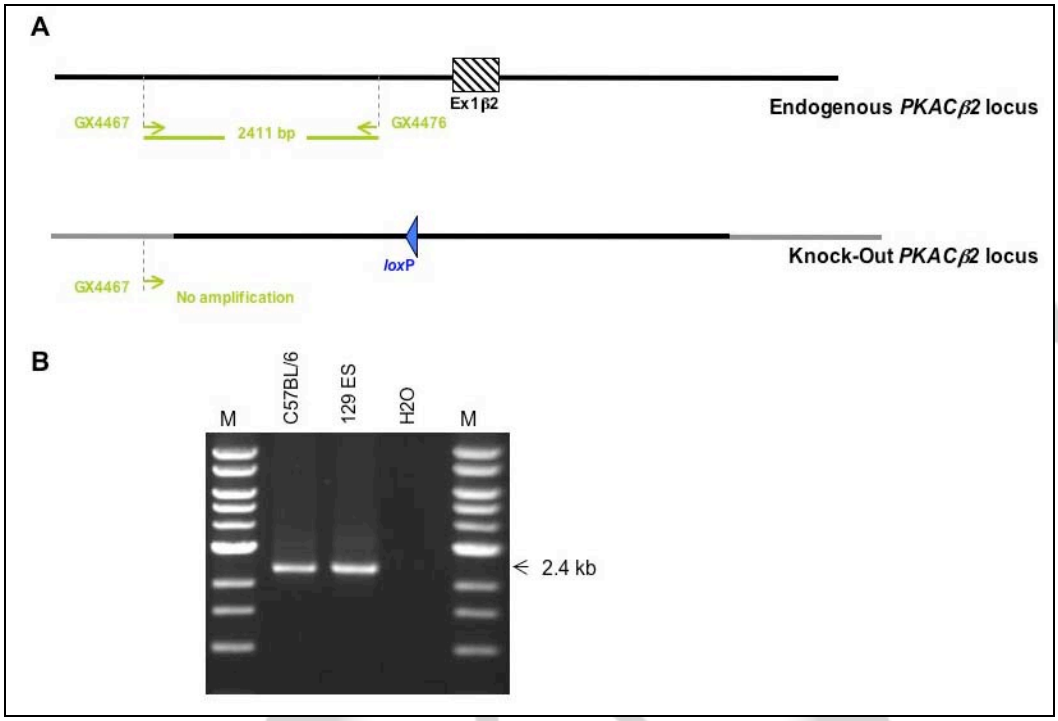

Figure 3: PCR identification of homozygous animals. *The figure indicates the PCR screening strategy for the detection of the knock-out PKACβ2 locus versus wild-type PKACβ2 locus. Green arrows illustrate the primers localisation.*

The primer pair GX4467/GX4476 has been designed and validated by genOway for the specific detection of the wild-type allele.

The forward primer GX4467 hybridises upstream of the short 5' homology arm. The reverse primer GX4476 is located within the 3' long homology arm in a region, which is deleted in Knock-out locus.

This set gives rise to a PCR product of 2.4 kb for the wild-type animals and the heterozygous animals and no product for the homozygous knock-out animals.

The sequence of the primers and the optimised PCR conditions are listed in tables 5 and 6.

Primer name	Primer sequence 5'-3'	Expected size of PCR product in	
		Wild-type allele	Knock-out allele
GX4467	CAATAGGTCCAACAGCCCATCTTGC	2411 bp	-
GX4476	TGTTGCTTGGCTAATGACTGTCAAAGC		

Table 5: Primers for the PCR screening for the detection of the *PKACβ2* wild type allele

Reaction mix			Reaction conditions			
Genomic DNA	10	ng	**Step**	**Temp.**	**Time**	**Cycles**
Primers	each 15	pmol	Denaturing	94°C	120s	1 x
dNTPs	0.5	mM	Denaturing	94°C	30s	35 x
Reaction buffer 3	0.1	Vol	Annealing	65°C	30s	
Expand HF Polymerase (Roche)	2.6	U	Extension	68°C	300s	
Reaction Volume	50.0	µl	Completion	68°C	480s	1 x

Table 6: Optimised PCR conditions for the detection of the *PKACβ2* wild type allele

Consequently, after F2 progeny PCR screening, signals are expected as shown on table 7:

Genotype of animals	PCR	Wild type allele	Knock-Out allele
Wild-type	GX4467/GX4476	2411 bp	/
	GX4473/ GX4474	5346 bp	/
Heterozygous	GX4467/GX4476	2411 bp	--
	GX4473/ GX4474	5346 bp	2551 bp
Homozygous	GX4467/GX4476	/	--
	GX4473/ GX4474	/	2551 bp

Table 7: Primers of the screening PCR

Altogether, the establishment of robust screening conditions secure the outcome of the project and provide the complete set of tools necessary for screening of animals along the development of the project.

Furthermore, as a general rule, once robust PCR screening is established, animals can be exclusively screened by PCR. However, as PCR remains a technique susceptible to produce artfactual signals, and in order not to loose the transgenic line, we would recommend to genotype by Southern blot all the animals used for breeding purpose.

1-4 SOUTHERN BLOT STRATEGY FOR THE GENOTYPING OF THE *PKACβ2* CONDITIONAL AND CONSTITUTIVE KNOCK-OUT LINES

The standard hybridisation conditions used at genOway are indicated below:

- Pre-hybridisation and hybridisation: 4 x SSC, 1 % SDS, 0.5 % skimmed milk, 20 mM EDTA, 100 μg/ ml hering sperm, at 65°C for 18 h.
- Washings: 2 times 3 x SSC, 1 % SDS at 65 °C for 15 min, then 2 times 0.5 x SSC, 1 % SDS at 65 °C for 15 min.
- Exposure: 3 days on BioMax MS films with BioMax intensifying screens.

As presented in the report sent on 25 August 2006, designed probes were BLASTed against murine genomic databases in order to select the probes with the best specificity based on *in silico* analysis. Moreover, in order to validate probe specificity, Southern blots were established using wild-type genomic DNA.

The strategy for Southern blot analysis is based on a BamHI/AflII digestion of the genomic DNA and hybridization with an internal 5' probe 5I-K, which leads to the detection of the following specific DNA fragments:

Allele	Expected size of BamHI/AflII fragment
Wild-type	9100 bp
Floxed	6435 bp
Knock-out	3482 bp

Table 8: Expected fragment sizes in Southern blot analysis

The 5' probe is generated by PCR on genomic DNA using the following primer pairs:

Primer name	Primer sequence 5' - 3'	Size of the probe
GX4643	GATAGACAGCCAGTATTAGTGTGACG	380 bp
GX4644	AGTAATACCACCAGGGTAGACAAGC	

Table 9: Primer pairs for the generation of the 5' probe

The Southern blot strategy as well as a representative example of a Southern blot analysis is documented in figure 4.

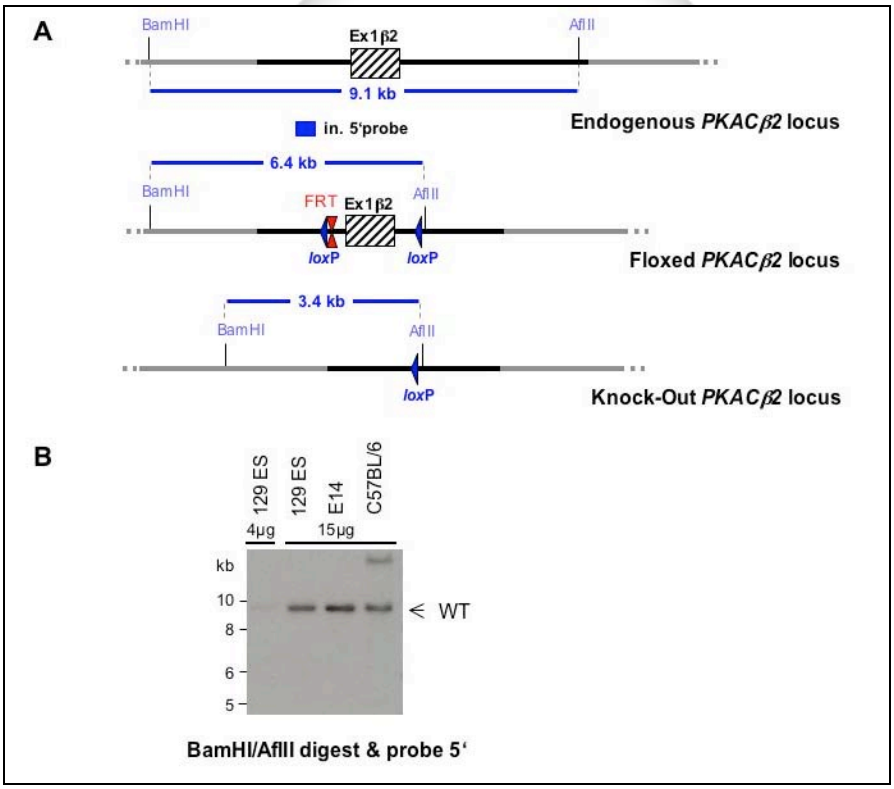

Figure 4: Southern blot analysis of the *PKACβ2* floxed and constitutive Knock-out lines. *(A) Schematic representation of the PKACβ2 wild-type, floxed and Cre-excised Knock-out allele with the relevant restriction sites for the 5' Southern blot strategy shown. (B) Result of the Southern blot tested with genomic wild-type DNA of 129Sv/Pas ES cells and C57BL/6 mouse tail DNA, each digested with BamHI/AflII. The digested DNA was blotted on nylon membrane and hybridised with the 5' probe detecting the BamHI/AflII -fragment of expected size in wild-type DNA. M: 1 kb DNA-Ladder (NEB)*

2 CONCLUSION

This report details the genotyping strategy for the generated *PKACβ2* floxed mouse line, carrying the *PKACβ2* exon 1β2 flanked by *loxP* sites, allowing the generation of a conditional Knock out line as well as the genotyping strategy for the constitutive *PKACβ2* Knock-out line, carrying the deletion of *PKACβ2* exon 1β2.

Should you encounter any difficulties in any of the proposed PCR and Southern blot experiments, please do not hesitate to let us know, so that we can assist you in the troubleshooting.

genOway successfully fulfilled its commitment with the generation of more than 2 conditional *PKACβ2* Knock-out mice. We would like to remind you that as stated in the general conditions of sales, genOway must be quoted in the "Materials and Methods" section for any publications related to the transgenic animal models developed by genOway services.

Should you have any comments when receiving this report, please let us know.

genOway - Head Office: 181 avenue Jean Jaurès • 69362 Lyon cedex 07 • France • Phone: +33 (0)4 37 65 41 00 • Fax: +33 (0)4 37 65 41 01
genOway Germany GmbH : Grundstrasse 16 • 20257 Hamburg • Germany • Phone: +49 (0)40 40 19 71 00 • Fax: +49 (0)40 43 20 82 61
e-mail: info@genoway.com • website: www.genoway.com